AN EVALUATION OF MICROBURST PREDICTION INDICES FOR THE KENNEDY SPACE CENTER AND CAPE CANAVERAL AIR STATION (KSC/CCAS)

THESIS

Steven N. Dickerson, Captain, USAF

AFIT/GM/ENP/00M-06

DEPARTMENT OF THE AIR FORCE
AIR UNIVERSITY

AIR FORCE INSTITUTE OF TECHNOLOGY

Wright-Patterson Air Force Base, Ohio

AFIT/GM/ENP/00M-06

AN EVALUATION OF MICROBURST PREDICTION INDICES FOR THE KENNEDY SPACE CENTER AND CAPE CANAVERAL AIR STATION (KSC/CCAS)

THESIS

Presented to the Faculty

Department of Engineering Physics

Graduate School of Engineering and Management

Air Force Institute of Technology

Air University

Air Education and Training Command

In Partial Fulfillment of the Requirements for the

Degree of Master of Science in Meteorology

Steven N. Dickerson, B.S.

Captain, USAF

March, 2000

APPROVED FOR PUBLIC RELEASE; DISTRIBUTION UNLIMITED

AFIT/GM/ENP/00M-06

AN EVALUATION OF MICROBURST PREDICTION INDICES FOR THE KENNEDY SPACE CENTER AND CAPE CANAVERAL AIR STATION (KSC/CCAS)

Steven N. Dickerson, B.S.
Captain, USAF

Approved:

Cecilia A. Miner (Chairman)	29 Feb 2000 date
Michael K. Walters (Member)	29 Feb 2000 date
David E. Weeks (Member)	29 Feb 2000 date
Daniel E. Reynolds (Member)	29 Feb 2000 date

The views expressed in this thesis are those of the author and do not reflect the official policy or position of the Department of Defense or the U. S. Government

Acknowledgements

There were many people to whom I am indebted; to list them all would be impossible. First, I would like to express my sincere appreciation to my thesis advisor Lt Col Cecilia Miner for her insight and advice throughout this research. I would also like to thank Professor Dan Reynolds for contributing his expertise in statistics to this research effort, and for opening his expansive library to me. I am also greatly indebted to Maj Gary Huffines for spending countless hours helping me write IDL programs even though he was not on my committee; without his help, I'd still be sitting in the weather lab.

I'd also like to thank Capt Ed Goetz for his help with discriminant analysis and for keeping me physically fit over the past year. Also deserving great thanks are Capt Jimmie Trigg, Lt Liz Boll, Lt Mike Holmes, and Pete Rahe for helping with the numerous formatting and programming problems I encountered.

Most importantly, I'd like to thank my wife Diane and my children Kevin and Amanda for their patience, and support during this research effort. Without your understanding this project would not have been possible.

Steven N. Dickerson

Table of Contents

List of Figures

List of Tables

Abstract

A wet-microburst event on 16 August 1994 at the Kennedy Space Center's Shuttle Landing Facility alerted forecasters from the 45th Weather Squadron (45WS), the provider of weather support to the Kennedy Space Center (KSC) and Cape Canaveral Air Station (CCAS), to the challenges of wet-microburst prediction. Although there was no operational impact, this event caused the 45WS to revise their severe thunderstorm forecasting procedures to specifically address microbursts, resulting in the locally developed Microburst-Day Potential Index (MDPI). MDPI provides a several-hour outlook of microburst potential based on the results of the Microburst and Severe Thunderstorm (MIST) project. The 45WS also conducted a preliminary evaluation of the Wind INDEX (WINDEX) for the KSC/CCAS microburst forecast problem. WINDEX provides an estimate of the maximum observed gust speed that can be expected should a microburst occur. This thesis presents an evaluation of MDPI and WINDEX based on microbursts identified by Sanger (1999) in his KSC/CCAS microburst climatology. A new index for assessing microburst potential is also introduced, incorporating both the MDPI and WINDEX parameters. Overall neither the MDPI nor the WINDEX performed particularly well in this application. The MDPI showed very little improvement over random guessing, and the WINDEX showed very little correlation to observed maximum microburst gust speed. The new microburst potential index outperformed MDPI in almost all categories. Further refinement of the new index is needed to make it a more useful forecasting tool.

AN EVALUATION OF MICROBURST PREDICTION INDICES FOR THE KENNEDY SPACE CENTER AND CAPE CANAVERAL AIR STATION (KSC/CCAS)

1. Introduction

1.1 Background

High winds are a significant hazard to space-launch operations, including movement of the space vehicle to the launch pad, the launch, Space Shuttle landing, and takeoff and landing of the Space Shuttle ferry aircraft. An unforecasted high wind event during any of these phases can be catastrophic, causing numerous casualties and severe damage to the space vehicle and launch pad. Less visible than the launch are the many support operations that can be adversely impacted by unforecasted strong wind events. Examples of such operations include fueling/defueling of the space vehicle, launch tower repair, erecting vehicles and payloads, space vehicle transportation, and flying operations.

One of the most difficult high wind events to predict is the downburst. A downburst is a strong thunderstorm downdraft that produces a "starburst" outflow of damaging wind at or near the surface. Downbursts have been sub-classified into two types: the macroburst and the microburst. A macroburst is a large downburst with damaging outburst winds extending horizontally more than 4 km (2.5 miles). Damaging winds from a macroburst can last from 5 to 30 minutes, with winds as high as 60 ms^{-1} (116 knots). Microbursts, on the other hand, are small downbursts with damaging

outburst winds not exceeding 4 km (2.5 miles) in horizontal extent. Microbursts generally last less than 10 minutes, with intense microbursts producing winds as high as 75 ms^{-1} (146 knots). Microbursts are further classified into "wet-microburst" and "dry-microburst" depending on the amount of precipitation associated with the downdraft (Fujita 1985). The small temporal and spatial scales of the microburst make them difficult to predict and pose a significant threat to space launch and support operations.

On 16 August 1994, the Kennedy Space Center (KSC) and Cape Canaveral Air Station (CCAS) experienced several "downrush" wind events. The strongest wind gust, which was in excess of 33.5 ms^{-1} (65 knots), was recorded at the Shuttle Landing Facility and was later attributed to a wet-microburst event (Wheeler and Roeder 1996). Forecasters assigned to the 45th Weather Squadron (45WS), the provider of weather support to Patrick Air Force Base (PAFB), the Kennedy Space Center, Cape Canaveral Air Station and the Eastern Range, forecasted airmass-type thunderstorm activity for that afternoon and expected high wind gusts but not near the magnitude that was experienced.

Although there was no operational impact, this event sparked the 45WS to launch a full investigation into how such a severe wind event could elude forecasters. As a result of the investigation, the 45WS created a conceptual forecast model, the "Microburst Funnel," to guide forecasters in microburst prediction (Figure 1).

The Microburst Funnel begins with a review of thunderstorm and microburst climatology for the KSC and surrounding area. If forecasters predict thunderstorm activity in the next 6 to 10 hours microburst outlook techniques, such as the Microburst-Day Potential Index (MDPI), and the Wind Index (WINDEX), are used to determine if the environment is favorable for microburst development, and to determine the maximum

wind gust that can be expected should a microburst occur. Intermediate techniques, such as satellite imagery interpretation, are used to identify areas where thunderstorm development is imminent. Finally, nowcasting techniques, such as radar and visual identification are used just prior to issuance or non-issuance of a high wind warning.

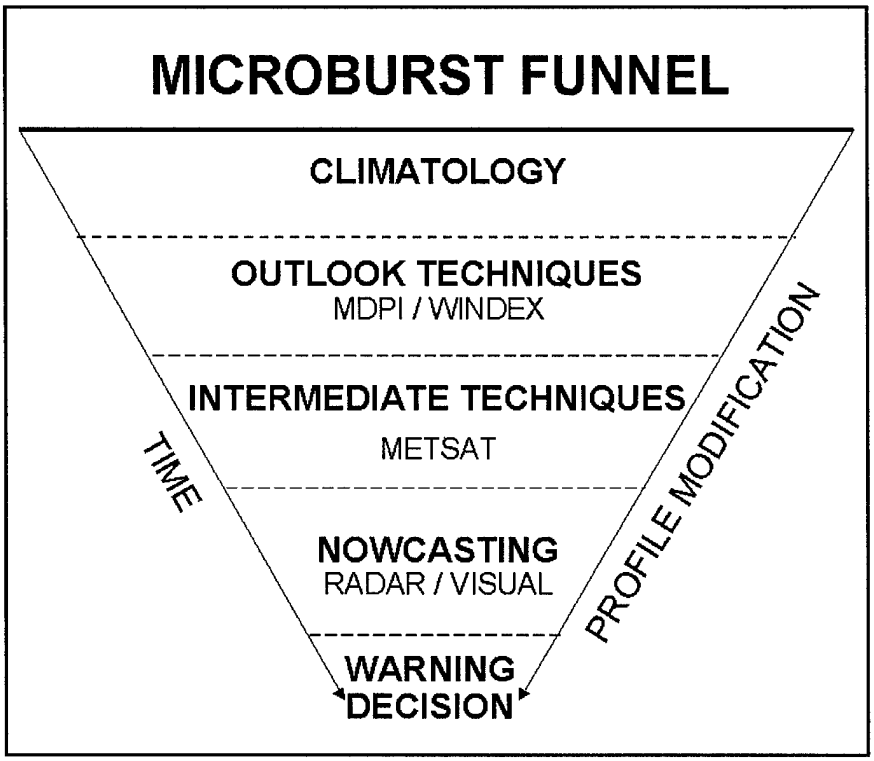

Figure 1. Microburst Funnel (Adapted from Roeder 1999)

This thesis focuses only on the two outlook techniques mentioned above, the MDPI and WINDEX indices, since most pre-launch operations, such as shuttle roll-out, can last up to eight hours. Early detection of a microburst producing environment in tandem with accurate microburst gust speed predictors can help mission planners postpone lengthy pre-launch operations when out-of-threshold winds are predicted, saving precious time and money.

Both MDPI and WINDEX are computed using upper-air sounding data. MDPI uses the difference between the minimum equivalent potential temperature (θ_e) found between 650 mb and 500 mb, and the maximum θ_e near the surface to assess the potential for microburst activity (Wheeler and Roeder 1996). WINDEX is an empirical index that gives an estimate of the maximum potential wind gust, at the surface, in knots (McCann 1994). Both indices are useful since they give significant lead time (6-10 hours) and are easily computed using data that is readily available.

Throughout this thesis, the terms "downburst" and "microburst" will be used interchangeably. This is common when the horizontal scale of the event is unknown (Caracena et al. 1990). All microbursts occurring at the KSC, CCAS, and Eastern Range will be assumed to be wet-microbursts since the thermodynamic requirements for dry-microbursts (an extensive, dry, sub-cloud layer) rarely exist on the Central Florida Atlantic Coast.

1.2 Problem Statement

Neither MDPI nor WINDEX have been evaluated by the 45WS for greater than a six month period. Additionally, neither index has been evaluated using the microburst cases identified by Sanger (1999) in his KSC/CCAS microburst climatology. Preliminary evaluation of MDPI indicated that $\Delta\theta_e$ values of greater than 30K suggest a high likelihood of a microburst, assuming thunderstorm or rainshower development. Evaluation of MDPI using a larger period of record is required.

Preliminary evaluation of the WINDEX caused the 45WS to question its usefulness at its locale. Expansion of the period of record is required before WINDEX

can be ruled out as a gust speed predictor for microbursts along the Central Florida Atlantic Coast. The 45WS is also interested in synergy between these two indices.

1.3 Objective

This thesis seeks to evaluate the MDPI by extending the evaluated data set from 6 months to 25 months (May-September 1994-1998).

A Weibull distribution is fit to 282 microburst gust speeds identified by Sanger (1999) in his KSC microburst climatology (see Chapter 2, section 2.6). The Weibull distribution is integrated for each of the 45WS warning thresholds, providing a "first guess" probability of needing to issue a convective wind warning should a microburst occur.

The WINDEX is also evaluated for its usefulness as a predictor of microburst gust speed for the Central Florida Atlantic Coast. Finally, a new index for assessing microburst potential is introduced. This new index incorporates both the MDPI and WINDEX variables.

1.4 Importance of Research

The 45WS provides weather support to launch and support activities conducted by the National Aeronautics and Space Administration (NASA), the Department of Defense (DOD), and other users of the CCAS, KSC, and Eastern Range launch facilities. Part of this support is issuance of convective wind warnings for the criteria listed in Table 1. The desired lead-times listed in Table 1 are needed to ensure PAFB, KSC, CCAS, and Eastern Range personnel have adequate time to protect valuable resources from adverse

weather. Failure to meet these lead-times may result in property loss and possible loss of human life. Accurate wind gust prediction indices play a vital role in helping to meet these stringent requirements.

Location	Criterion	Lead-time
KSC (Sfc-300ft)	≥ 35 knots ≥ 50 knots ≥ 60 knots	30 minutes 60 minutes 60 minutes
CCAS (Sfc-200ft)	≥ 35 knots ≥ 50 knots	30 minutes 60 minutes
PAFB (Sfc)	≥ 35 knots ≥ 50 knots	60 minutes 60 minutes

Table 1. Convective Wind Warning Criteria (Roeder 1999)

1.5 Overall Approach

Six steps were required to complete this research. First a Weibull distribution was fit to 282 microburst gust speeds identified by Sanger (1999) in his KSC microburst climatology. This distribution was integrated for each of the 45WS convective wind warning thresholds, providing a "first guess" of the probability of breaking a threshold should a microburst occur. Second was the identification of microburst-days and the identification of thunderstorm-days without microbursts. This was accomplished by identifying all thunderstorm-days for the KSC and CCAS between May - September 1994-98 by analyzing surface observations from the KSC and CCAS. A day was considered a "thunderstorm-day" if the KSC or CCAS surface observation reported thunderstorms, rainshowers, cumulonimbus, or lightning in either the significant weather section or the remarks section. These days were cross-referenced with the KSC/CCAS microburst-days identified by Sanger (1999) in his KSC microburst climatology. Since Sanger did not identify microburst events for 1994 a computer program was written to identify microbursts occurring in May-September 1994.

Step three consisted of computing the MDPI and WINDEX parameters. CCAS sounding data furnished by the Air Force Combat Climatology Center was used to compute MDPI and WINDEX values.

Step four consisted of a performance evaluation of both the MDPI and WINDEX equations. Statistical tools such as hit-rate, false-alarm rate, probability of detection, Heidke skill score, and the Pearson correlation coefficient (r) were used to measure the performance of each index.

Step five was development of a new microburst potential index using the MDPI and WINDEX parameters by way of discriminant analysis. Lastly, a performance comparison between the original MDPI and the new microburst potential index was completed using the same performance measurements listed in step three.

1.6 Organizational Overview

Chapter 2 presents an overview of literature regarding convective downbursts, including a brief history of terminology and the development of the MDPI and WINDEX indices. Chapter 3 describes the data set used in this thesis and the computation of the MDPI and WINDEX parameters. Chapter 4 discusses the research methodology. The statistical techniques used for data analysis and development of a new microburst index are also covered. Chapter 5 summarizes the results and conclusions, and discusses opportunities for future research.

2. Literature Review

2.1 A Brief History of Microburst Terminology

How have meteorologists gone from downdraft to "microburst?" The best way to answer this question is to look at the events, or discoveries, that led to this term. The existence of downdrafts, associated with thunderstorms, has been known to meteorologists since the late 19th century (Fujita and Caracena 1977). The most notable study of horizontal and vertical air currents in and around thunderstorms, the Thunderstorm Project, was conducted by Byers and Braham (1949) in the late 1940's. Based on this project, Byers and Braham (1949) established the three stages of thunderstorm cells that are commonly taught at universities around the world: a) the cumulus stage characterized by updrafts throughout the cell, b) the mature stage with both updrafts and downdrafts, and c) the dissipating stage dominated by strong downdrafts. Downbursts are a special type of downdraft first categorized in the mid-1970's.

While investigating the Eastern Airlines Flight 66 crash that occurred at John F. Kennedy Airport, New York City on 24 June 1975, Dr. T. Theodore Fujita hypothesized that the accident was a result of a unique wind phenomenon that he called a "downburst" (Fujita and Caracena 1977). Fujita defined a downburst as a downdraft with speeds "comparable to or greater than the approximate rate of descent or climb of a jet aircraft on the final approach or takeoff at 91 m (300 ft) above the surface." He chose what he considered a conservative threshold value of 3.6 m s^{-1} (12 ft s^{-1}) as the dividing line between an ordinary downdraft and a downburst.

In 1978, the first field research project on downbursts, the Northern Illinois Meteorological Research On Downburst (NIMROD), was conducted by the University of Chicago, and was headed by Fujita and Srivastava (Fujita 1985). Using three Doppler radars and 27 portable automated mesonet stations, the research team collected data on a large number of downbursts over a period of 42 days. Because of the overwhelming number of wind observations recorded during the 42 day period (approx. 1,632,960 observations), Fujita (1985) developed a computer algorithm for identifying potential downbursts that occurred within the network (Table 2). Condition 1 sets a minimum gust speed of 10 ms^{-1} (19.4 knots) to be considered a downburst. Conditions 2 and 3 state that the peak wind must be at least 5 ms^{-1} (10 knots) faster than the five-minute mean wind speed prior to and after the peak wind. Conditions 4 and 5 ensure that the peak wind is not a gust "superimposed" on sustained high winds. Condition 6 excludes the gust front "which is characterized by an exponential decay of the gusty winds behind a front" (Fujita 1985).

Condition 1	Peak wind must be greater than 10 ms^{-1} (19.4 knots)
Condition 2	Peak wind must be at least 5 ms^{-1} (10 knots) faster than five-minute mean prior to peak
Condition 3	Peak wind must be at least 5 ms^{-1} (10 knots) faster than five-minute mean after the peak
Condition 4	Peak wind must be 1.25 times the five-minute mean prior to the peak
Condition 5	Peak wind must be 1.25 times the five-minute mean after the peak
Condition 6	Five-minute mean prior to peak must be no more than 1.5 times the five-minute mean after the peak

Table 2. Six Condition Algorithm for Identifying Potential Downbursts (Fujita 1985)

To obtain further evidence of a downburst, Fujita (1985) simultaneously plotted wind vectors for all towers at the time of the suspected downburst in order to analyze the field for a distinctive divergent flow pattern. A potential downburst was catagorized as a true downburst only if a divergent flow pattern was recognized. Fifty downbursts were identified during this project.

Noticing significant differences in the horizontal scale of these downbursts, Fujita (1985) subclassified them into "macroburst" and "microburst." A macroburst is a large downburst with damaging outburst winds extending horizontally more than 4 km (2.5 miles). Damaging winds from a macroburst can last from 5 to 30 minutes, with winds as high as 60 ms^{-1} (116 knots). Microbursts, on the other hand, are small downbursts with damaging outburst winds not exceeding 4 km (2.5 miles) in horizontal extent. Microbursts generally last less than 10 minutes, with intense microbursts producing winds as high as 75 ms^{-1} (146 knots) (Fujita 1985).

Of the 50 microbursts detected during the NIMROD field project, 64% were accompanied by 0.25 mm (0.01 inches) of rain or more. The remaining 36% had no measurable rain. Because of this, microbursts were further classified into "dry microburst" and "wet-microburst" depending on the accompaniment of measurable rain (Fujita 1985). Since then, research by Brown et al. (1982), Caracena et al. (1983), Wakimoto (1985), and many others, has helped to increase understanding of the dry microburst environment. Wet-microbursts have not been studied nearly as much; however, it is clear that the wet-microburst environment is quite different from the dry-microburst environment (Caracena et al. 1990).

2.2 Wet-Microburst Storm Structure

In 1975, a meteorological mesonetwork was established in south central Florida for the Florida Area Cumulus Experiment (FACE). The FACE project was not a microburst study; however, on 1 July 1975, a wet-microburst made nearly a direct hit on the experiment's Field Observing Site (FOS). Weather observers at the FOS originally believed that a tornado had touched down nearby. An investigation shortly after the storm determined that the damage pattern was indicative of outflow at the base of a downdraft versus flow into a tornado vortex (Caracena and Maier 1987). Because of the fine data resolution of the collected data, and the central location of the microburst within the mesonetwork, this microburst, known as the FACE microburst, has significantly enhanced current understanding of wet-microburst structure (Caracena and Maier 1987).

Generally, thunderstorms producing wet-microbursts are characterized by low cloud bases, storm tops reaching as high as 15 km (49,000 ft) and strong precipitation cores that are composed almost entirely of ice in the upper-levels (Atkins and Wakimoto 1991). They normally occur in environments that are nearly moist adiabatic and statically unstable from the surface to about 500 mb, with a deep layer of high relative humidity near the surface (Doswell 1994). This rather moist layer is capped by a cool, dry layer (low equivalent potential temperature) which is the most probable source of microburst energy once convection and precipitation begin to occur (Caracena and Maier 1987). As downdrafts from precipitation loading begin, the cool, dry layer ejects pockets of dry air into the saturated downdraft region (Caracena et al. 1990). Latent heat of evaporation into the dry air contributes significantly to the negative buoyancy of the parcel (Caracena and Maier 1987). The key to developing a wet-microburst is this

evaporation of condensed water during descent, thus maintaining saturation. Without this evaporation, the parcel would begin to warm at the dry adiabatic lapse rate, become warmer than its surrounding environment, and quickly lose its negative buoyancy (Doswell 1994). Figure 1 shows a schematic of a thunderstorm producing a wet-microburst. In addition to the evaporative effects, the presence of high relative humidity in the low levels increases the virtual temperature difference between the downdraft and the environment, also contributing to an increase in negative buoyancy (Atkins and Wakimoto 1991).

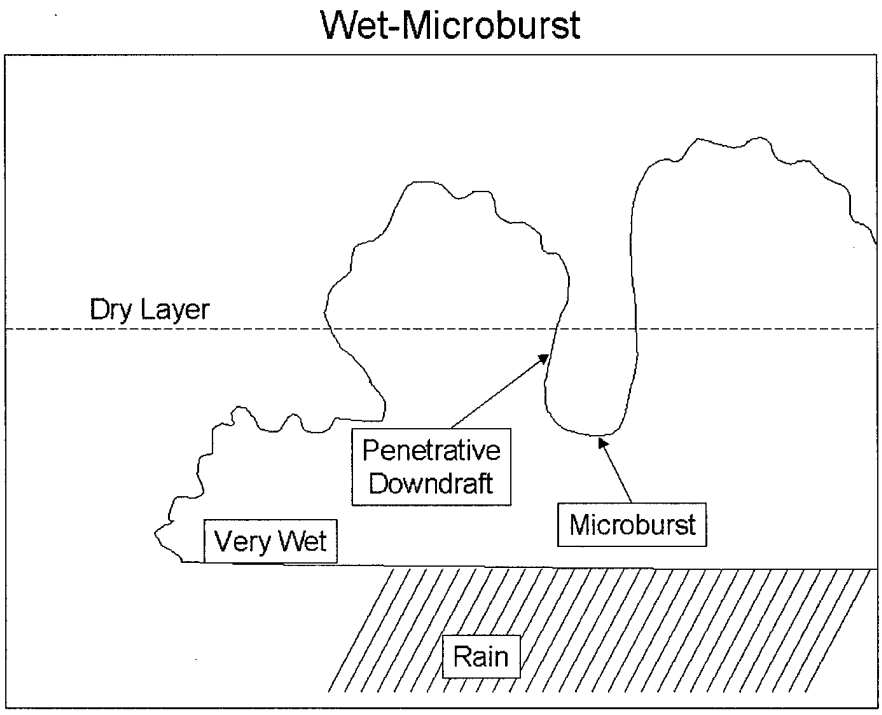

Figure 2. Conceptual model of a wet-microburst characterized by a dry source layer that ejects dry pockets of air into an underlying saturated layer, producing the evaporation that can cause a microburst (After Caracena et al. 1990).

2.3 The Wet-Microburst Environment

Using data collected during the Microburst and Severe Thunderstorm (MIST) project that operated in northern Alabama in 1986, Atkins and Wakimoto (1991) documented the general environmental conditions (thermodynamic characteristics) that favor wet-microburst development. The MIST project used a network of 41 Portable Automated Mesonet (PAM-II) stations and 30 FAA-Lincoln Laboratory Operational Weather Studies (FLOWS) stations, spaced approximately 2 km (1.25 miles) apart, to collect meteorological data every minute. Atmospheric soundings were also taken twice daily, one at 0700 CDT, and one at 1300 CDT. From this set of data, 33 microbursts were identified using a computer algorithm first suggested by Fujita (1985). Analyzing the synoptic charts, sounding data, and mesonetwork data from the MIST network area, Atkins and Wakimoto (1991) determined the thermodynamic characteristics for microburst-producing days and compared them to the characteristics for the days with thunderstorms that did not produce microbursts.

Atkins and Wakimoto described a wet-microburst environment as one that begins with a shallow morning radiation inversion that inhibits convection in the lowest 75 mb of the atmosphere. As the surface begins to heat, the inversion is replaced by a dry-adiabatic sub-cloud layer that extends from the surface to about 850 mb. The layer between 850 mb and 500 mb is relatively moist. This is capped by a cool, dry layer above 500 mb (Atkins and Wakimoto 1991). Figure 2 shows morning and afternoon sounding models for a wet-microburst-producing day.

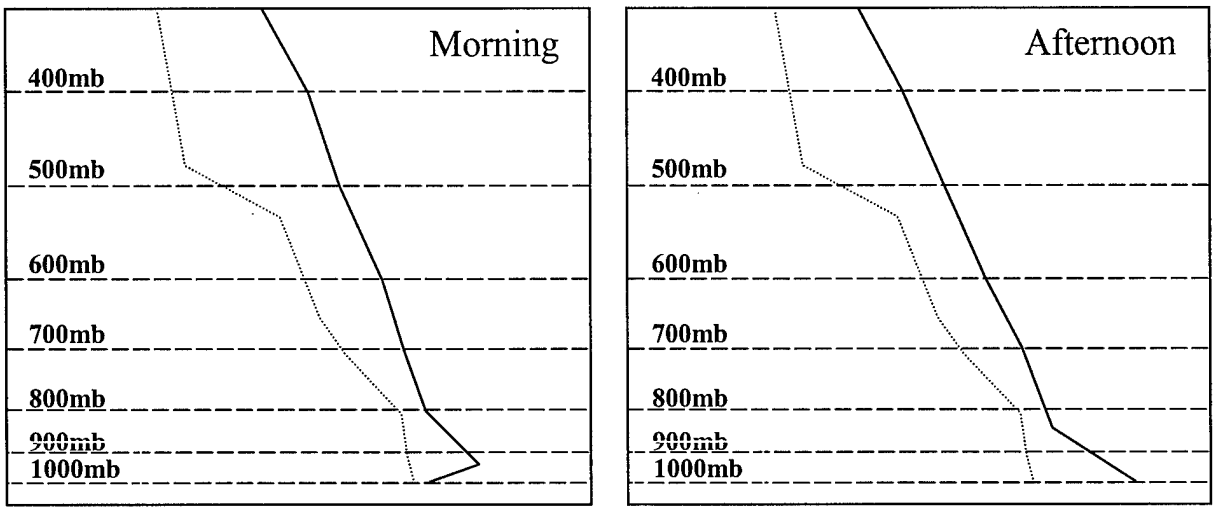

Figure 3. Model Thermodynamic Charts Conducive for Wet-Microburst Occurrence. Dashed line is the dew point curve; solid line is the temperature curve (After Atkins and Wakimoto, 1991).

By plotting the equivalent potential temperature (θ_e) profiles for the microburst producing days, Atkins and Wakimoto found a minimum of θ_e was typically found between 650 mb and 500 mb, or just below the capping cool, dry layer. The afternoon θ_e profile showed a $\Delta\theta_e$, from the surface to the mid-level minimum, greater than or equal to 20 K. The non-microburst producing storms had a $\Delta\theta_e$ less than or equal to 13 K. Equivalent potential temperature plots for other well-documented wet-microburst cases confirmed these results. Atkins and Wakimoto then suggested that by forecasting an afternoon sounding based on the morning sounding, the $\Delta\theta_e$ values of 20 K and 13 K can be used as "threshold" values for the development of wet-microbursts. They envisaged these thresholds being used to issue a general "area-wide alert" for potential wet-microburst activity. Figure 4 shows model morning and afternoon θ_e profiles for a wet-microburst environment.

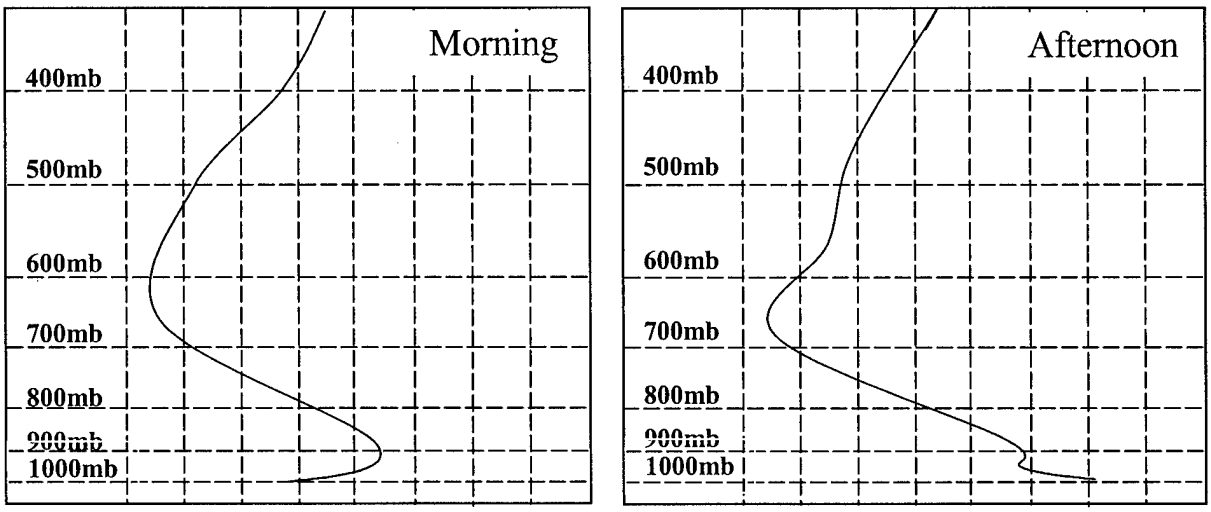

Figure 4. Model θ_e profile (solid curve) for an environment conducive to wet-microburst development. Vertical dashed lines are θ_e values increasing from left to right at a 5 K interval (After Atkins and Wakimoto 1991).

2.4 The Microburst-Day Potential Index (MDPI)

A wet-microburst event that occurred at the Kennedy Space Center's (KSC) Shuttle Landing Facility on 16 August 1994 led the 45WS to revise their severe thunderstorm forecasting procedures to specifically address microbursts. This resulted in the development of the Microburst-Day Potential Index (MDPI). MDPI provides a several-hour outlook of microburst potential based on θ_e profiles first introduced by Atkins and Wakimoto (1991). The MDPI equation is:

$$MDPI = \frac{Maximum\,\theta_e - Minimum\,\theta_e}{CT} \qquad (1)$$

where

Maximum θ_e is the maximum θ_e in the lowest 150 mb of the sounding (Kelvin)

Minimum θ_e is the minimum θ_e in the layer between 650 and 500 mb (Kelvin), and

CT is the critical threshold (or normalization factor) currently defined as 30 K.

Given thunderstorm development, MDPI values of 1 or greater indicate a strong probability of a wet-microburst, and MDPI values of less than 1 indicate a low probability of a wet-microburst. Preliminary analysis of MDPI indicated that it shows good skill in alerting forecasters to the potential for wet-microbursts (POD = 96.4%) without an unreasonable false alarm rate (FAR = 32.5%) (Wheeler and Roeder 1996).

2.5 The Wind INDEX (WINDEX)

McCann (1994) introduced an index for identifying airmasses favorable for the development of microbursts. The "Wind INDEX," or WINDEX, is based on studies of observed and modeled microbursts. It is a highly empirical index based on the vertical momentum and continuity equations developed by Wolfson (1990). Wolfson showed that microburst vertical velocity is proportional to some "forcing" times the depth of the downdraft (Δz). "This forcing is proportional to the square of the environmental lapse rate, Γ, through which a downdraft descends (McCann 1994)." Since a major source of microburst negative buoyancy is from the absorption of latent heat due to melting and evaporation, McCann considers the downdraft depth to be the height of the melting level above the surface. The WINDEX equation is:

$$WI = 5[H_M R_Q(\Gamma^2 - 30 + Q_L - 2Q_M)]^{0.5} \quad (2)$$

where

H_M is the height of the melting level above the ground (km)

Γ is the lapse rate from the surface to the melting level (°C km^{-1})

Q_L is the mixing ratio of the lowest 1 km above the surface (g kg^{-1})

Q_M is the mixing ratio at the melting level (g kg^{-1})

N is the moisture adjustment 12 g kg^{-1}, and

$R_Q = Q_L/N$ but not exceeding 1.

Before using WINDEX, it is important to consider the following: 1) When the lapse rate is low, the radicand may become negative. When this happens, WI is zero and the probability of a microburst is nil. 2) The term R_Q attempts to account for an overestimation of WINDEX values in a dry environment. This term implies that when the low-level mixing ratio is less than 12 g kg^{-1}, the atmosphere is too dry to produce a high precipitation storm. 3) WINDEX is very sensitive to environmental lapse rate error. 4) Multiplication of the radicand by five, on the right side of the WINDEX equation, gives an estimate of the maximum potential surface gust in knots (McCann 1994).

WINDEX is computed using observed sounding data or data from numerical prediction models. The actual WINDEX value is the maximum potential surface gust, in knots, that can be expected from a microburst (McCann 1994). Based on McCann's verification data, WINDEX correlates well with the observed gust speeds of known microburst events. Table 3 shows WINDEX values and observed gust speeds for well documented microbursts.

LOCATION	DATE	WINDEX	OBSERVED	SOURCE
Southern FL	1 Jul 75	53	60	Caracena and Maier (1987)
Northern AL	20 Jul 86	59	60	Wakimoto and Bringi (1988)
Northern AL	13 Jul 86	56	56	Wakimoto and Bringi (1988)
San Antonio, TX	2 Sep 87	63	59	Ladd (1989)
San Antonio, TX	2 Sep 82	68	53	Ladd (1989)
Norman, OK	26 Aug 87	54	55	Stewart (1991)
Tampa, FL	19 Jul 88	56	52	Stewart (1991)
Vero Beach, FL	4 Jun 90	61	50	Stewart (1991)
Amarillo, TX	21 May 86	44	47	Sohl (1987)
near Denver, CO	19 May 82	47	48	Wakimoto (1985)

Table 3. WINDEX Calculations for Known Microburst Events (McCann 1994).

Preliminary analysis of WINDEX by the 45WS showed that it tends to underestimate gust speeds for the Central Florida Atlantic Coast (Roeder 1999). Further analysis is required to determine the usefulness of WINDEX at the KSC and CCAS.

2.5.1 Forcasting Dry Microbursts Using WINDEX

Murdoch (1997) evaluated WINDEX as a gust predictor for dry-microbursts in the Southwest United States. Dry-microbursts were identified using Storm Data (1983-1993) and other dry-microburst studies. Nineteen upper-air soundings taken at 12 UTC between the months of March - October, from Midland, Amarillo, and El Paso, Texas and Albuquerque, New Mexico were loaded into the Skew-T/Hodograph Analysis and Research Program (SHARP) workstation for analysis. The 19 soundings were provided by the National Climatic Data Center (NCDC) and from the National Weather Service Office (NWSO) Midland's upper-air data archives. Once loaded into SHARP, the soundings were modified to reflect the conditions at the time of the microburst. These "modified" soundings were used to calculate WINDEX.

Murdoch (1997) concluded that WINDEX "agreed well with the observed and estimated wind gusts, yeilding a mean error of -5.8 [knots]." Murdoch (1997) offered two explanations for this underestimation in cases where the cloud bases were high: 1) Loss of momentum as the absorption of latent heat ends and adiabatic heating continues, and 2) Low average 1 km mixing ratios compared to a typical dry microburst sounding.

2.5.2 WINDEX Computation from Weather Satellite Derived Soundings

The National Environmental Satellite Data and Information Service (NESDIS) Forecast Products Development Team (FPDT) evaluated two experimental microburst prediction products derived from Geostationary Operational Environmental Satellite (GOES) sounder retrievals (vertical temperature and moisture profiles) (Ellrod and Nelson 1998). One of the experimental products plots WINDEX as a color-coded graphic superimposed on a visible, infrared, or water vapor image. This product was evaluated for a two-month period. WINDEX values were compared to reports of wind damage or wind gusts greater than 50 knots reported in the National Weather Service (NWS) Storm Prediction Center's (SPC) preliminary storm data. More than 300 wind damage reports were compared to adjacent WINDEX values derived from sounder retrievals. In 92 percent of the cases WINDEX values were greater than 40 knots, while 60 percent exceeded 50 knots. Overall, Ellrod and Nelson (1998) found that the absolute value of the mean GOES WINDEX differed from the mean observed wind gusts by less than 3 knots. They found that the GOES WINDEX product was "generally most reliable over the eastern and central United States during daylight hours" (Ellrod and Nelson 1998).

2.6 Microburst Identification at the Kennedy Space Center (KSC)

A four-year, summertime microburst climatology was produced for the KSC, CCAS, and Eastern Range by Sanger (1999). This is the first microburst climatology ever produced in the United States. The period of record was May through September 1995-98. A total of 282 microbursts were identified over 114 microburst days during this

four-year period. Sanger showed that the most prominent months with microbursts, within the KSC WINDS network, are June, July, and August with the highest frequency in July. "The most favorable time for microbursts is between 1600 UTC (12 P.M. EDT) and 2200 UTC (6 P.M. EDT) with the peak occurring between 2000 UTC (4 P.M. EDT) and 2200 UTC (6 P.M. EDT)" (Sanger 1999). Appendix A lists the microburst events identified by Sanger.

2.6.1 The KSC/CCAS Weather Information Network Display System (WINDS)

The KSC operates one of the densest mesonetworks in continuous operation in the United States. This network collects, disseminates, and archives wind direction and speed, as well as other meteorological parameters, over an area of approximately 1200 km^2 which encompasses the KSC, CCAS, Eastern Range, and surrounding remote locations. On average there is one tower every 27 km^2. The most densely instrumented region is along the East Coast within the KSC, CCAS, and Eastern Range complexes (Figure 5). The instrumented towers that make-up this network take meteorological measurements every minute, but archive data at five-minute intervals. Therefore, the data used for Sanger's (1999) research consisted of the peak and mean wind speeds every five-minutes verses the one-minute interval used in the NIMROD and MIST studies (Sanger 1999).

Sanger (1999) mentions several limitations of the WINDS network that make microburst identification difficult. First is the overall placement of the towers. Sanger mentions that many of the towers have "poor meteorological exposure" resulting in erroneous data. Second is the overall tower spacing. Towers to the south and southwest of CCAS are sparsely populated potentially inhibiting detection of a microburst between

towers. Third is the varying number of sensors on each tower. Some towers may only have sensors at 6 and 30 feet (Tower 512) while others may have as many as 8 sensors at 6, 12, 54, 162, 204, 295, 394, and 492 feet (Tower 3131). Lastly, Sanger believes that the data interval of five-minutes may be too long for identifying short-lived microburst events (Sanger 1999).

2.6.2 Microburst Identification Technique

Sanger (1999) used a computer program, written in the Interactive Data Language (IDL), to analyze WINDS tower data from May through September 1995-98 to identify possible microbursts. Six conditions (Table 4) needed to be met simultaneously before a wind reading could be considered a possible microburst event. These conditions are a modified version of Fujita's (1985) six condition algorithm for identifying potential downbursts. Since the WINDS archive data interval is 5 minutes, the pre-peak mean wind speed and post-peak mean wind speed used by Fujita were replaced by the peak wind 5 minutes before and 5 minutes after the potential microburst.

Condition 1	Potential microburst must be greater than 10 ms^{-1} (19.4 knots)
Condition 2	Potential microburst must be at least 5 ms^{-1} (10 knots) faster than the five-minute peak prior to the potential microburst
Condition 3	Potential microburst must be at least 5 ms^{-1} (10 knots) faster than the five-minute peak after the potential microburst
Condition 4	Potential microburst must be 1.25 times the five-minute peak prior to the potential microburst
Condition 5	Potential microburst must be 1.25 times the five-minute peak after the potential microburst
Condition 6	Five-minute peak prior to potential microburst must be no more than 1.5 times the five-minute peak mean after the potential microburst

Table 4. Sanger's Six Condition Algorithm for Identifying Potential Microburst (Sanger 1999)

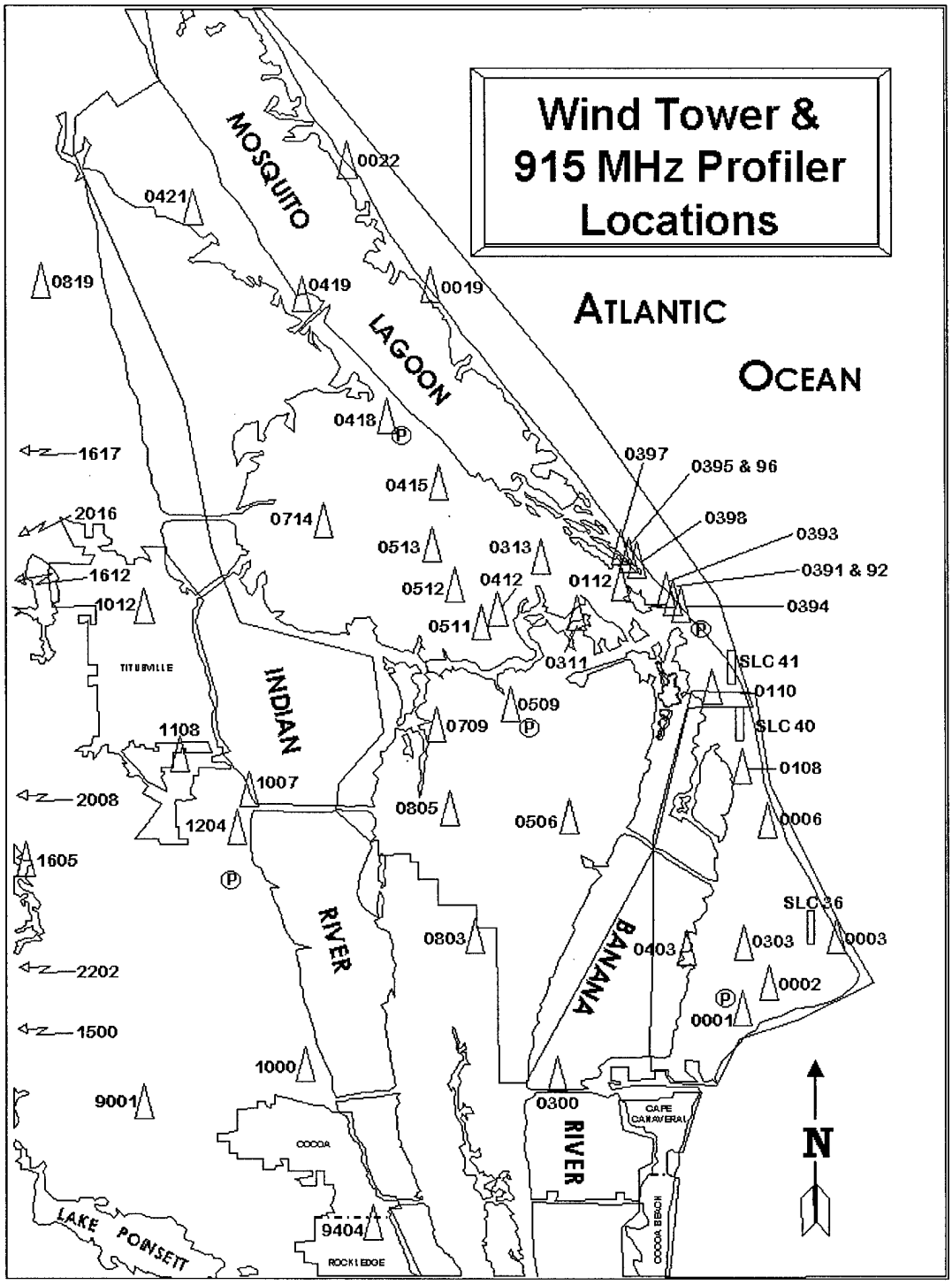

Figure 5. Map of KSC WINDS Tower Network. Triangles indicate tower location.

Like Fujita, Sanger simultaneously plotted wind vectors for all towers at the time of the suspected microburst in order to analyze the field for a distinctive divergent flow pattern. Sanger, however, did not throw-out a suspected microburst if a divergent flow pattern could not be identified, noting that the wide spacing of towers could miss the divergent flow pattern. This is consistent with the technique used in the 1986 MIST project (Atkins and Wakimoto 1991).

3. Data and Computation of MDPI and WINDEX Parameters

3.1 Introduction

Three data-sets were used to accomplish this research: a) Weather Information Network Display System (WINDS) tower data from May - September 1994, b) Upper-air sounding data from May - September 1994-98, and c) KSC and CCAS surface observations from May - September 1994-98. The following gives a brief description of these data-sets and an overview of how they were used in the context of this research.

3.2 Weather Information Network Display System (WINDS) Tower Data

The Weather Information Network Display System (WINDS), operated by the KSC, collects, disseminates, and archives data from 201 meteorological sensors on 44 instrumented towers at the CCAS and KSC, and at remote surrounding sites. This network is one of the most dense mesonetworks in continuous operation in the United States, covering approximately 1200 km^2 for an average of one tower every 27 km^2. These towers are organized into three groups based on their primary application (Raytheon 1996):

a. Launch Critical Towers - These towers are at the launch complexes, the Shuttle Landing Facility (SLF) and in some remote locations. They use the most sensitive sensors in the network and are used to ensure that launch constraints are satisfied during countdown and major pad operations. These sensors are also used to assess possible blast damage effects due to detonation of the solid rocket motors.

b. Safety Critical Towers - These towers are located near areas where propellants and other toxic chemicals are stored or handled. They are used by Range Safety models to predict the diffusion of potential airborne contaminants released from chemical spills.

c. Forecast Critical Towers - These towers generally surround the KSC and CCAS, and are used primarily for weather forecasting and early detection of hazardous weather conditions.

It is important to mention that, although each tower is assigned to one of the above groups, the data from these towers is displayed and archived as one integrated network, allowing any tower to contribute to any application. The distinction between tower groups is, therefore, insignificant operationally (Raytheon 1996).

Of primary concern for this research are the wind speeds and gust speeds recorded by this network. WINDS data for May - September 1994 was provided by the 45WS in the format shown in Appendix B. The following parameters were provided: Julian Day, time (UTC), tower number, sensor height (ft), mean wind direction (degrees), 5-minute average wind speed (knots), instantaneous peak speed recorded in a 5-minute interval (knots), standard-deviation of wind direction (degrees), temperature (°C), dew-point temperature (°C), and relative humidity (%). Not all sensors report all of the above parameters. This data was used to identify potential microbursts that occurred in 1994, using Sanger's six condition algorithm for identifying potential microbursts (Sanger 1999).

3.3 KSC Upper-Air Sounding Data

Upper-Air Sounding Data from the KSC (station 74794) for the period May - September 1994-98 was provided by the Air Force Combat Climatology Center.

Soundings are taken routinely during the summer months at the KSC, at 10 UTC, 15 UTC, and 22 UTC. Additional soundings are taken on launch days, and on days with highly weather sensitive operations. The MDPI and WINDEX parameters were computed using the 15 UTC soundings since most microbursts, at KSC, occur between 16 UTC and 22 UTC (Sanger 1999). The 10 UTC sounding is too early and would have little predictive ability for microbursts that occur after 16 UTC. Use of the 22 UTC sounding would have virtually no predictive ability since most microbursts occur before this time. The sounding data provided includes the following: date, time, geopotential height, pressure level, temperature, dew-point temperature, wind direction, and wind speed. Missing data is indicated by a "999" entry. Appendix C is a sample upper-air sounding in decoded format. Column 1 is the time (UTC); column 2 is the day; column 3 is the month; column 4 is the year; column 5 is the pressure (mb); column 6 is the height (meters); column 7 is the temperature (°C); column 8 is the dew-point temperature (°C); column 9 is the wind direction (degrees); column 10 is the wind speed (knots).

3.3.1 Handling Missing Data Within a Sounding

Many of the WINDEX and MDPI parameters require temperature and/or dew-point temperatures for levels that were reported as missing (reported as "999"). A computer program, written in IDL, was used to interpolate this data (Appendix D). Interpolation was done by assuming a constant lapse rate from the last known temperature (or dew-point) to the next known temperature (or dew-point) in the sounding. Figure 6 illustrates this interpolation process.

Step 1 takes the difference between the last known and next known temperatures in the sounding. Step 2 computes the difference between the height of the last known

temperature value and the next known temperature value in the sounding. Step 3 builds a weighting ratio by taking the ratio of the difference between the height of the missing temperature value and the value computed in Step 2. This weighting ratio ensures that the temperature used in place of the missing value is proportional to the change in height from the last known temperature. Step 4 multiplies the weighting ratio by the value computed in Step 1 and subtracts that value from the last known temperature, yielding the interpolated temperature value. This same process is used to interpolate missing dew point temperatures as well.

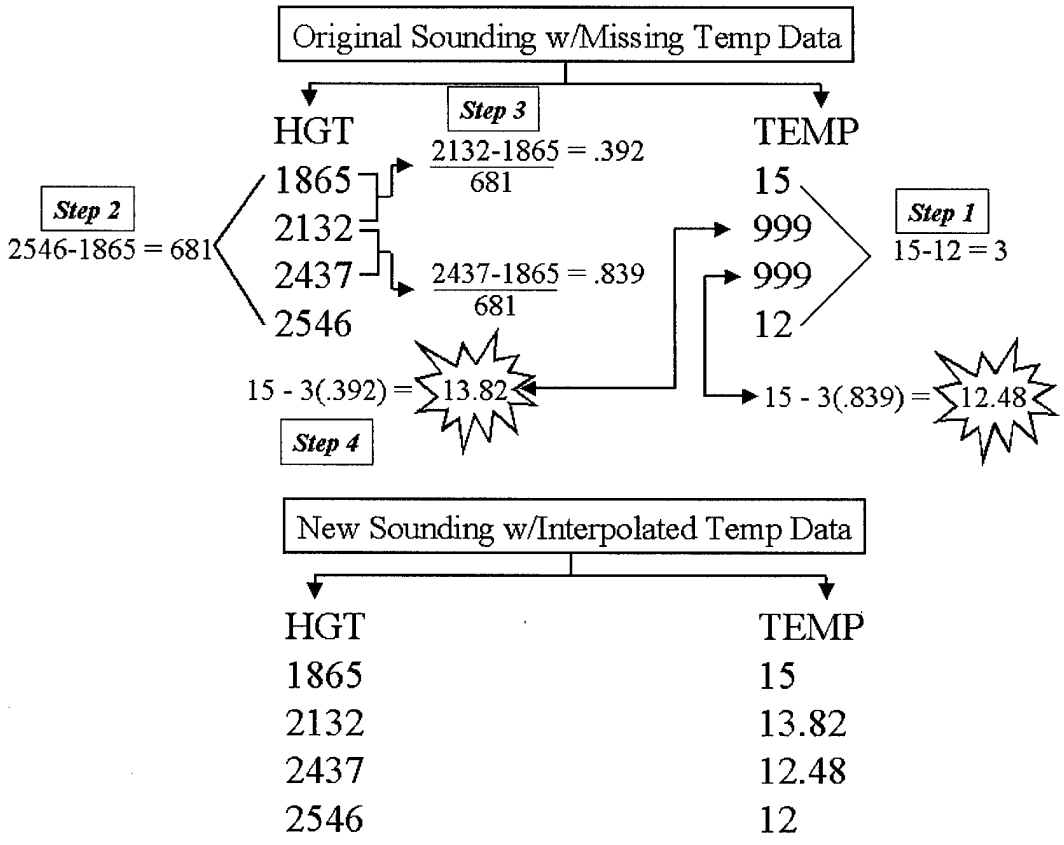

Figure 6. Interpolation of Missing Temperature Data. A weighting ratio was computed and then multiplied by the change in temperature between the two known levels. This value was then subtracted from the last known temperature reading. This ensured that the temperature was reduced by an amount that was proportional to the change in height from the last known temperature to the height of the missing value.

3.3.2 Computation of the MDPI parameters

The Microburst-Day Potential Index uses the difference in equivalent potential temperature between the surface (lowest 150 mb) and mid-levels (between 650 mb and 500 mb) to determine the potential for microburst activity within the next 6-10 hours. Equivalent potential temperature (θ_e) is the temperature a parcel of air would be if it was expanded pseudo-adiabatically until all the water vapor has condensed, released its latent heat, and fallen out, and was then compressed dry-adiabatically to 1000 mb (Wallace and Hobbs 1977). The following equations, from *AWS/TR-83/001 Equations and Algorithms for Meteorological Applications in Air Weather Service* (Duffield and Nastrom 1983), were used to compute equivalent potential temperature:

$$\theta_e = T\left[\left(\frac{P_o}{P}\right)^{k(1-0.28w)}\right]\exp\left[\left(\left(\frac{A}{T_{LCL}}\right)-2.54\right)w(1+0.81w)\right] \tag{3}$$

where

$$T_{LCL} = T_d - (B + 0.001571T_d - 0.000436T_o)(T_o - T_d) + C \tag{4}$$

and

θ_e is the equivalent potential temperature (Kelvin)

T is the temperature at pressure level P (Kelvin)

P_o is the reference pressure level 1000 mb

P is pressure (mb)

A is the empirically derived value 3376 K

T_{LCL} is the temperature at the lifted condensation level (LCL) (Kelvin)

k is 0.2854

w is the mixing ratio (kg kg^{-1})

B is the empirically derived value 0.212 °C

C is the value 273.16 K which converts Celsius to Kelvin

T_d is the surface dew point temperature (°C), and

T_o is the surface temperature (°C)

A computer program written in the Interactive Data Language (IDL) was used to compute θ_e at each level of the atmospheric sounding (Appendix D). The following equations were used to compute the mixing ratio (w) needed in equation (3):

$$w = 0.622 \cdot \frac{e}{p - e} \tag{5}$$

where

$$e(T_d) = D \cdot \exp\left[\frac{17.67 \cdot T_d}{T_d + E}\right] \tag{6}$$

and

w is the mixing ratio (kg kg^{-1})

p is the pressure at the level where T is measured (mb)

e is the vapor pressure at the level where T_d is measured (mb)

D is the empirically derived value 6.112 mb

E is the empirically derived value 243.5 °C

T_d is the dew-point temperature at the level where T is measured (°C)

Equation (6) approximates the vapor pressure, and is valid within 0.1% over the temperature range -30°C $\leq T_d \leq$ 35°C (Rogers and Yau 1996).

3.3.3 Computation of the WINDEX Parameters

WINDEX uses five parameters that are computed from an atmospheric sounding, to estimate the maximum gust speed at the surface that can be expected from a microburst. These parameters are the height of the melting level (H_m) (km), the mean environmental lapse rate from the surface to the height of the melting level (Γ) (°C km^{-1}), the mixing ratio in the lowest 1 km of the atmosphere (Q_l) (g kg^{-1}), the mixing ratio at the melting level (Q_m) (g kg^{-1}), and a moisture adjustment factor (R_q) which is equal to Q_l/12 but not greater than 1. A computer program written in IDL was used to compute WINDEX (Appendix D). The following is a brief overview of how each parameter was computed:

a. Height of the Melting Level (H_m) - The height where the temperature sounding first becomes less than zero (McCann 1999). This height was converted to kilometers by dividing by 1000.

b. Mean Environmental Lapse Rate (Γ) from the Surface to H_m - This was computed by dividing the surface temperature by the height of the melting level (H_m) (McCann 1999).

c. Mixing Ratio in the Lowest 1 km (Q_l) - Computed by using equations (5) and (6), above, to compute the mixing ratio at the surface and at 1 km. The arithmetic mean was then computed and used as Q_l.

d. Mixing Ratio at the Melting Level (Q_m) - Computed by using equations (5) and (6), above, at the level where the temperature sounding first becomes less than zero.

e. Moisture Adjustment Factor (R_q) - This is equal to $Q_l/12$ but not greater than 1.

3.4 KSC and CCAS Surface Observations

Surface observations from the KSC (KCOF) and the CCAS (KTTS), for the period May - September 1994-98, were used to identify thunderstorm days. A day was considered a "thunderstorm-day" if the KSC or CCAS surface observation reported thunderstorms, rainshowers, cumulonimbus, or lightning in either the significant weather section or the remarks section between 15 UTC and 22 UTC. These days were cross-referenced with the KSC/CCAS microburst-days identified by Sanger (1999), in his KSC microburst climatology, to determine which days had thunderstorms that produced microbursts and which days had thunderstorms that did not produce microbursts.

4. Methodology

4.1 Introduction

This thesis seeks to accomplish four objectives for the 45WS. 1) Fit a Weibull distribution to the 282 microburst gust speeds identified in Sangers's (1999) KSC microburst climatology and integrate for the 45WS convective wind warning criteria. 2) Evaluate MDPI using an expanded period of record. 3) Evaluate WINDEX as a predictor of microburst gust speed for the KSC/CCAS microburst forecast problem. 4) Develop a new microburst index using the MDPI and WINDEX parameters. The methodology presented in this chapter was designed to meet these objectives accurately and efficiently.

4.2 Summary of Methodology

1) Fit a Weibull Distribution to the KSC/CCAS observed microburst gusts identified by Sanger (1999) and integrate for convective wind warning criteria.

2) Identify 1994 microburst cases and add to Sanger's climatology.

3) Distinguish microburst producing thunderstorm days from non-microburst producing thunderstorm days.

4) Compute MDPI and WINDEX parameters.

5) Evaluate MDPI using standard forecast verification techniques (i.e., probability of detection, false alarm rate, hit rate, threat score, Heidke skill score).

6) Compare WINDEX versus observed microburst gust speed to determine predictive value.

7) Use WINDEX and MDPI parameters to develop a new microburst potential index by way of discriminant analysis.

8) Compare new index to MDPI using standard forecast verification techniques.

4.3 Fitting a Weibull Distribution to the KSC Microburst Climatology

In 1939, the Swedish physicist Waloddi Weibull introduced a family of distributions now known as Weibull distributions. In some instances there are theoretical justifications for the use of a Weibull distribution, but in many applications they simply provide the best fit of observed data. The probability density function (pdf) for a Weibull distribution is

$$f(x;\gamma,\alpha,\beta) = \begin{cases} \frac{\alpha}{\beta^{\alpha}}(x-\gamma)^{\alpha-1}e^{-\left(x-\gamma/\beta\right)^{\alpha}} & x \geq 0 \\ 0 & x<0 \end{cases} \qquad (7)$$

where

x is the range of the observed data

γ is the offset (equal to 0 if distribution begins at the origin)

α is the shape parameter

β is the scale parameter

Weibull distributions are fit to a data set by adjusting the offset, shape and scale parameters to fit the distribution of the observed data (Devore 1995). Crystal Ball© was used to obtain the shape and scale parameters that fit the gust speed distribution of the 282 microbursts identified by Sanger (1999). Mathcad© was then used to integrate

equation (7) for the 45WS convective wind warning criteria yielding the probability of having microburst gusts greater than 35 knots, 50 knots, and 60 knots. Figure 7 is a sample Weibull distribution with $\gamma = 15$, $\alpha = 2$, and $\beta = 30$.

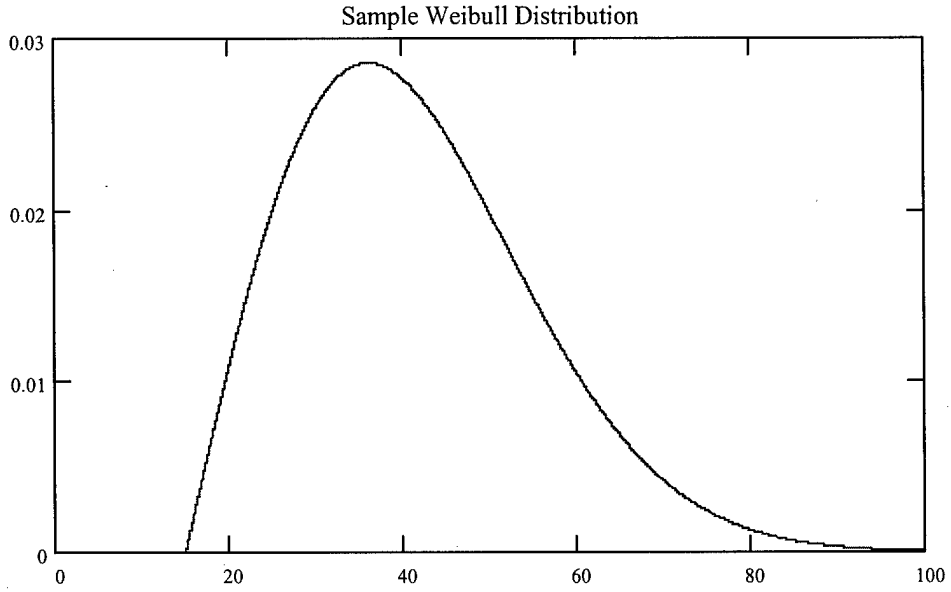

Figure 7. Sample Weibull Distribution with $\gamma = 15$, $\alpha = 2$, and $\beta = 30$.

4.4 Identifying 1994 Microbursts Using WINDS Tower Data

WINDS tower data was provided by the KSC for May - September 1994. A program written in IDL was used to identify microbursts based on Sanger's (1999) six-condition algorithm since these microbursts would be added to his climatology. Three hundred seventy-two potential microbursts were identified using this approach. Further analysis of the data indicated that an overwhelming majority of these "microbursts" were a result of an apparent archival problem with the 1994 data. Thirty-four of the potential microbursts had peak gusts greater than 90 knots even though Sanger identified only 2 microbursts with winds greater-than or equal-to 90 knots in his 4-year climatology. Most

of the extremely high peaks (70 knots or greater) had 5-minute mean winds, for the same period, of less than 10 knots. Additionally, many towers that have multiple sensors indicated a high peak wind at one level that was not reflected at levels above or below. Table 5 is a sample erroneous "microburst" from the 1994 WINDS data. Notice the peak wind of 117 knots at 54 feet with a mean during the same period of only 3 knots. Such a high peak wind should have a more significant influence on the mean for the same period. Additionally, the peak wind reading at 12 feet (just 42 feet below the "microburst"), for the same tower and period, is only 14 knots.

Julian Date	Time	Tower	Height	Direction	Mean	Peak
94142	1215	112	12	330	3	14
94142	1215	112	54	333	3	117

Table 5. Sample Erroneous Microburst. The 117-knot peak wind at 54 feet should have greater influence on the 5-minute mean for that height and the peak wind at 12 feet for the same period.

"Microbursts" like the one described in Table 6 plagued the 1994 WINDS data, making it impossible to distinguish real microbursts from erroneous data. It is believed that these anomalies are an archival problem since the errors are not isolated to just a few towers and heights. As a result, the 1994 tower data was discarded and not added to Sanger's (1999) climatology.

4.5 Distinguishing Microburst/Non-Microburst Thunderstorm Days

Surface observations from the KSC (KCOF) and the CCAS (KTTS), for the period May - September 1994-98, were used to identify thunderstorm days. A day was considered a "thunderstorm-day" if the KSC or CCAS surface observation reported

thunderstorms, rainshowers, cumulonimbus, or lightning in either the significant weather section or the remarks section between 15 UTC and 22 UTC. These days were cross-referenced with the microburst-days identified by Sanger (1999), in his KSC microburst climatology, to determine which days had thunderstorms that produced microbursts and which days had thunderstorms that did not produce microbursts.

4.6 Computing MDPI and WINDEX Parameters

The MDPI and WINDEX parameters were computed for microburst and non-microburst days that had 15 UTC soundings available. All parameters were computed using the equations and procedures described in Chapter 3. Of the 114 microburst-days identified by Sanger (1999), 92 had microbursts between 15 UTC and 22 UTC; of those, 73 had 15 UTC soundings available. One hundred sixty-seven non-microburst producing thunderstorm days had thundertorms between 15 UTC and 22 UTC, and 15 UTC soundings available. Appendix E lists the MDPI and WINDEX parameters for the 240 microburst and non-microburst producing thunderstorm days used in this study.

4.7 Evaluating MDPI

The MDPI was evaluated using the following forecast verification methods: probability of detection (POD), false alarm rate (FAR), hit rate (HR), threat score (TS), and Heidke skill score (HSS). These are the same methods used in previous MDPI studies conducted by the 45WS. A chi-squared (χ^2) test for goodness of fit was also computed for completeness. Additionally, a scatterplot of $\Delta\theta_e$ versus microburst occurrence was used to evaluate the MDPI critical threshold (CT).

Table 6 is a generic 2 X 2 contingency table used for forecast verification. Each position on the table displays the absolute frequencies, or counts, of each possible combination of forecast and observed pairs. Dividing these counts by the sample size (total number of forecast/observed pairs) transforms the counts into relative frequencies (Wilks 1995). The equations for computing the following accuracy and skill measures refer to Table 6.

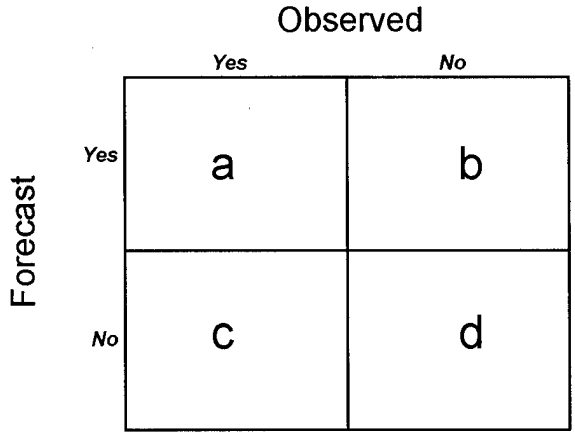

Table 6. 2 X 2 Contingency Table for Forecast Verification (After Wilks 1995)

4.7.1 Probability of Detection (POD)

The probability of detection (POD), also known as prefigurance, is the fraction of occasions in which the forecast event occurred when it was forecast. For this study it is the likelihood that a microburst would be forecast, given that it occurred. The best possible POD is 1, indicating all microbursts that occurred were forecast. The worst POD is 0, indicating all microbursts that occurred were not forecast (Wilks 1995). In terms of Table 6

$$POD = \frac{a}{a+c} \tag{8}$$

4.7.2 False Alarm Rate (FAR)

The false alarm rate (FAR) is the proportion of forecasts for which the forecasted phenomenon fails to materialize. For this thesis, it is the likelihood that a microburst is forecast but not observed. The best possible FAR is 0, indicating that all forecast microbursts were observed. The worst possible FAR is 1, indicating none of the forecast microbursts were observed (Wilks 1995). In terms of Table 6

$$FAR = \frac{b}{a+b} \tag{9}$$

4.7.3 Hit Rate (HR)

The hit rate (HR), sometimes known as the proportion correct, is the fraction of the total forecasts that are correct. The worst hit rate is zero and the best hit rate is 1. The HR is sometimes multiplied by 100% and called the percent correct (Wilks 1995). In terms of Table 6

$$HR = \frac{a+d}{n} \tag{10}$$

where n is the total number of forecast/observation pairs (a+b+c+d).

4.7.4 Threat Score (TS)

Sometimes it is not always desirable to use HR as a measure of forecast accuracy since it credits "yes" and "no" forecasts equally. The threat score (TS), or critical success index (CSI), is often used when the event to be forecast, in this case microburst occurrence, occurs substantially less frequently than the non-occurrence. Essentially, the TS "is the number of correct "yes" forecasts divided by the total number of occasions on which that event was forecast and/or observed" (Wilks 1995). This is basically the same

as removing the correct "no" forecasts from the hit rate. The lowest attainable threat score is 0 and the best is 1 (Wilks 1995). In terms of Table 6

$$TS = CSI = \frac{a}{a+b+c} \tag{11}$$

4.7.5 Heidke Skill Score (HSS)

Equations (8), (9), (10), and (11) measure the average correspondence between a forecast and the event the forecast is trying to predict. They are measurements of accuracy but not skill. Forecast skill is a measure of the relative accuracy of a set of forecasts, based on a set of control or reference forecasts. To have skill, the forecasts must perform better than the reference forecasts. The Heidke skill score (HSS) is a measure of forecast skill using the hit rate that would be achieved by random chance as the reference. It is the most commonly used skill score for summarizing 2 X 2 contingency tables. Perfect forecasts receive a HSS of 1, forecasts that are as good as the reference receive a HSS of 0, and forecasts that perform worse than the reference receive a negative HSS (Wilks 1995). HSS is computed in terms of Table 6 by

$$HSS = \frac{2(ad-bc)}{(a+c)(c+d)+(a+b)(b+d)} \tag{12}$$

4.7.6 Chi-Squared Test for Goodness of Fit

To assess the validity of a forecast technique it is important to determine how the observed "hits" and "misses" in a 2 X 2 contingency table compare to the "hits" and "misses" that would be generated by a completely random selection process. The method for assessing the validity of the forecast technique is a chi-squared (χ^2) test for goodness of fit. The null hypothesis for the χ^2 test is that the forecasts do not perform better than a

random selection process; the researcher's hypothesis is that the forecasts do perform better than a random selection process (Kachigan 1986). The equation for computing χ^2 is

$$\chi^2 = \sum_{\text{all cells}} \frac{(\text{observed} - \text{expected})^2}{\text{expected}} \tag{13}$$

where the expected value is computed by multiplying the marginal totals for the row and column, corresponding to the particular cell, and then dividing by the sum of all cells (n). In terms of Table 6 the expected value of cell a is

$$\text{expected value of cell } a = \frac{(a+b)(a+c)}{a+b+c+d} \tag{14}$$

If the χ^2 value is greater than a critical value determined by an a priori significance level (α) then the null hypothesis is rejected and the forecast technique is said to be valid. If the χ^2 value is less than the critical value the forecast technique is said to be without merit (Kachigan 1986).

P-values were also computed based on the χ^2 value. The *p*-value is the area under the χ^2 distribution to the right of the χ^2 value. It is the smallest level of significance (α) at which the null hypothesis would be rejected. The *p*-value can also be thought of as the probability of getting a χ^2 value greater than or equal to the one obtained by the sample data, given the null hypothesis is true. For example, if a χ^2 value of 8.15 is computed based on a 2 X 2 contingency table, the associated *p*-value of 0.0043 would indicate that there is a 0.43% probability of obtaining that value given the null is true (Devore 1995).

4.7.7 Evaluating MDPI Critical Threshold (CT)

The MDPI critical threshold was evaluated using a scatterplot of $\Delta\theta_e$ versus microburst occurrence. The $\Delta\theta_e$ was plotted on the ordinate and microburst occurrence was plotted on the abscissa. Microburst occurrence was plotted as a 1 and non-occurrence was plotted as a 0. Figure 8 is an idealized scatterplot of $\Delta\theta_e$ versus microburst occurrence. Note that ideally there is very little overlap between the $\Delta\theta_e$ values corresponding to microburst occurrence and the $\Delta\theta_e$ values corresponding to non-microburst occurrence, with the overlap centered roughly on the MDPI critical threshold (30K - horizontal line).

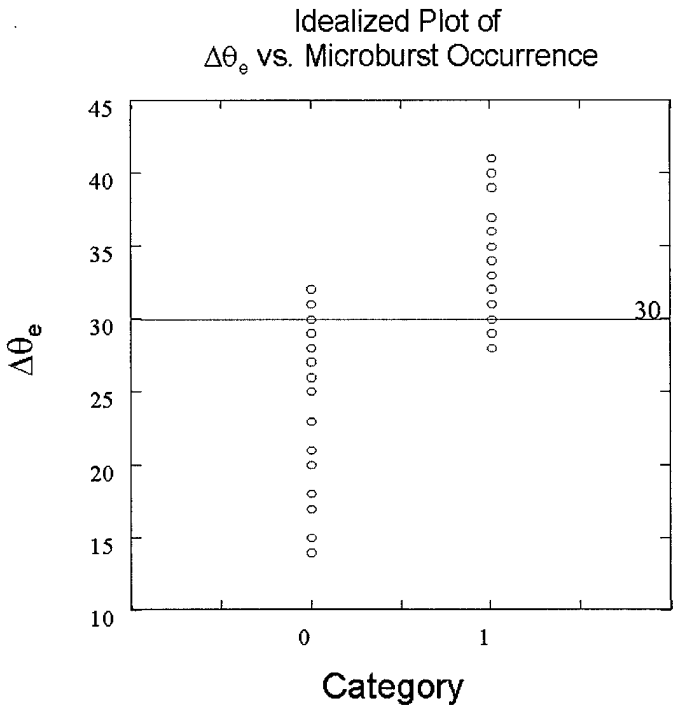

Figure 8. Idealized Plot of $\Delta\theta_e$ vs. Microburst Occurrence. Microburst occurrence is plotted as a 1 and non-microburst occurrence is plotted as a 0. Horizontal line marks the MDPI critical value (30K).

4.8 Evaluating WINDEX

The Pearson correlation coefficient (r) was used to evaluate the degree of association between the maximum gust speeds predicted by WINDEX and the observed microburst gust speeds identified by Sanger (1999). Commonly referred to as the correlation coefficient, r is used to determine if there is a linear relationship between two variables. The value of r is bound by 1 and -1, with 1 indicating a perfect positive correlation, 0 indicating no correlation, and -1 indicating a perfect negative correlation (Wilks 1995). The equation for computing the Pearson correlation coefficent for n pairs $(x_1,y_1),\ldots,(x_n,y_n)$ is

$$r = \frac{s_{xy}}{\sqrt{\sum (x_i - \bar{x})^2}\sqrt{\sum (y_i - \bar{y})^2}} \tag{15}$$

where

$$s_{xy} = \sum_{i=1}^{n} (x_i - \bar{x})(y_i - \bar{y}) \tag{16}$$

For the purpose of this thesis, 73 (n=73) WINDEX/observed gust speed pairs $\{(x_i,y_i),\ldots,(x_{73},y_{73})\}$ were evaluated. The WINDEX was computed using the 15 UTC soundings for microburst days identified by Sanger (1999). These WINDEX values were paired with the maximum microburst gust speed observed between 15 UTC and 22 UTC for the given microburst day.

A scatterplot of observed maximum microburst gust speed versus WINDEX was used to visually determine the degree of linear correlation and to see if a non-linear relationship exists. Figure 9 shows an idealized scatterplot of observed maximum microburst gust speed versus WINDEX. The correlation coefficient for the idealized plot

is 1. Notice that the plot increases from left to right at a 45 degree angle showing a perfect linear relationship.

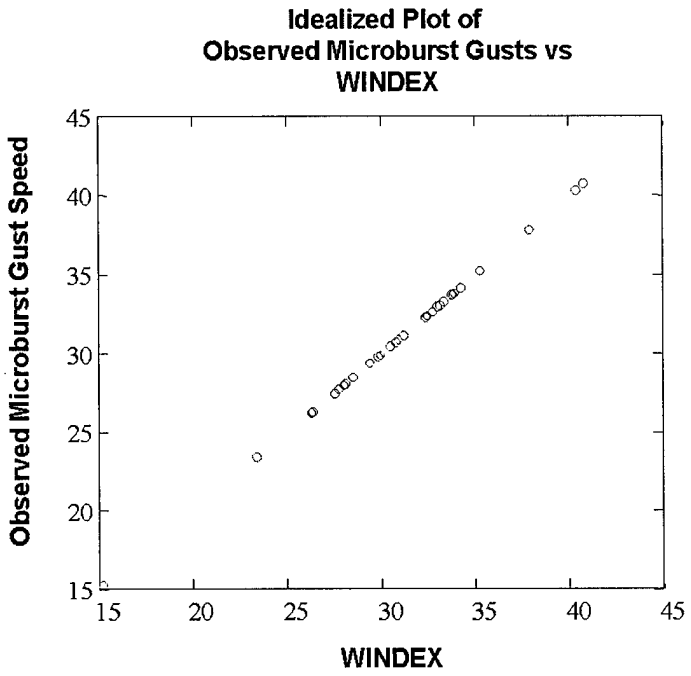

Figure 9. Idealized plot of observed maximum microburst gust speed versus WINDEX. The plot increases from left to right at a 45-degree angle indicating a perfect positive correlation ($r = 1$).

4.9 New Index Development

A statistical technique known as discriminant analysis was used to develop a new index for assessing wet-microburst potential for the Central Florida Atlantic Coast. Discriminant analysis is a method of classifying individuals or objects into mutually exclusive and exhaustive groups based on a set of independent predictor variables. It involves deriving linear combinations of the predictor variables that will discriminate between two or more previously defined groups such that misclassification error is minimized (Dillon and Goldstein 1984). This is done by assigning discriminant weights to the predictor variables. A discriminant score for each measured object is calculated by

multiplying the discriminant weight, associated with each predictor variable, by the object's value on the predictor variable and then summing over the set of predictor variables. The equation for computing the discriminant scores is known as the discriminant function. For n number of objects to be classified and p predictor variables the discriminant function has the form

$$\mathbf{Y}=\mathbf{b}'\mathbf{X} \tag{17}$$

where

$\mathbf{Y}$ is a $1 \times n$ vector of discriminant scores

$\mathbf{b}'$ is a $1 \times p$ vector of discriminant weights, and

$\mathbf{X}$ is a $p \times n$ matrix containing the values for each of the n objects on the p predictor variables.

Objects are then grouped based on their discriminant scores and a discriminant cutoff score. Discriminant scores above the cutoff are placed into one group; discriminant scores below the cutoff are placed into the other. Figure 10 shows a graphical illustration of a two-group discriminant analysis with two predictor variables. The top part of the graph depicts a scatterplot of the two predictor variables (X_1 and X_2) for each object in the two groups. The lower part of the graph depicts the Y distributions (distributions of discriminant scores) for the two groups. The dotted line separating the two groups and two distributions is the cutoff score. Note that the greater the overlap of the two Y distributions (or scatterplots) the more errors in classification (Dillon and Goldstein 1984).

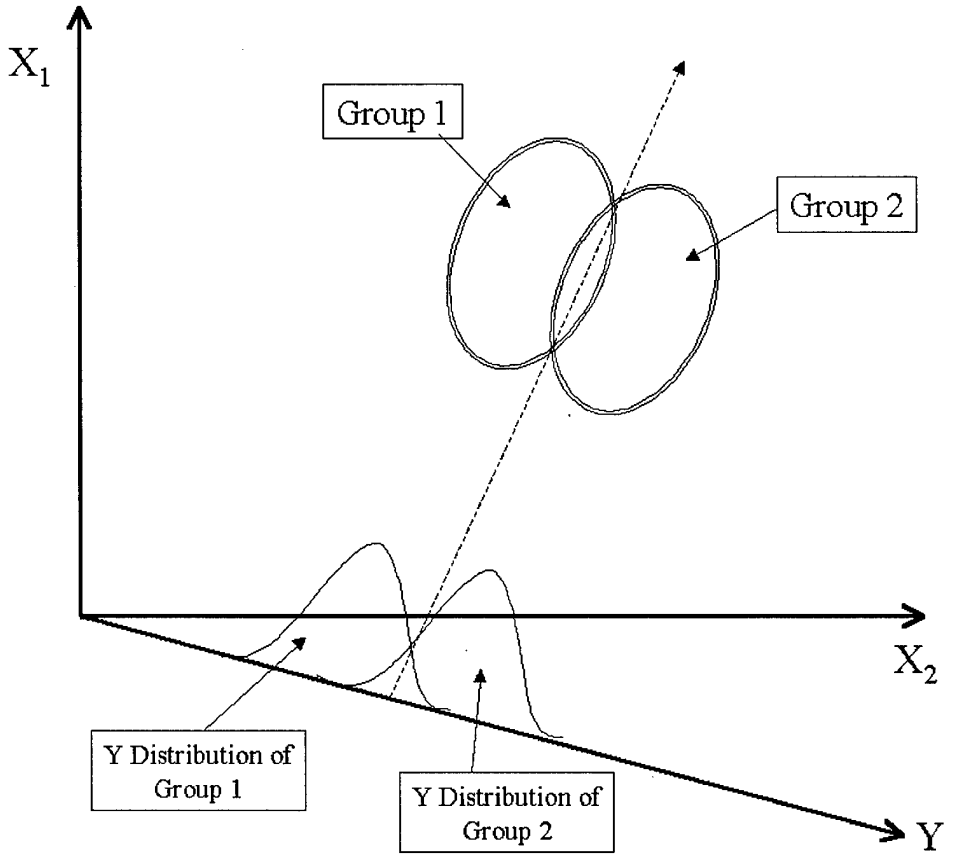

Figure 10. Graphical Illustration of Two-Group Discriminant Analysis. The upper part of the figure depicts a scatterplot (enclosed by ovals) of the two predictor variables (X_1 and X_2). The lower portion of the figure depicts the distributions of discriminant scores (Y) for each group (After Dillon and Goldstein 1984).

There were six steps to developing a new index using discriminant analysis. They were 1) choose predictor variables from the pool of MDPI and WINDEX parameters and other atmospheric measurements related to computing MDPI and WINDEX, 2) build a discriminant analysis input table (matrix) to train the discriminant model, 3) determine the discriminant weights, 4) compute discriminant scores for each group and determine the best cutoff score, 5) develop and evaluate the confusion matrix, and 6) compare the performance of the discriminant function (new index) to MDPI.

4.9.1 Choosing Predictor Variables

For the purpose of this thesis, the two groups being discriminated were microburst producing thunderstorm days and non-microburst producing thunderstorm days. The predictor variables were drawn from the pool of MDPI and WINDEX parameters and other MDPI and WINDEX related variables. The nine MDPI and WINDEX parameters are described in Chapter 3. Other atmospheric parameters used as potential predictor variables were

a. The pressure corresponding to the maximum θ_e in the lowest 150 mb of the atmosphere (mb) ($P_{max\theta e}$)

b. The pressure corresponding to the minimum θ_e between 650 mb and 500 mb (mb) ($P_{min\theta e}$). This is an indicator of the height of the cool, dry layer based on MDPI.

c. The minimum θ_e regardless of the pressure level (K) ($Min\,\theta_{e\text{-}actual}$). This is the value used to compute $\Delta\theta_e$ in the MIST project (Atkins and Wakimoto 1991).

d. The pressure corresponding to $Min\,\theta_{e\text{-}actual}$ (mb) ($P_{min\theta e\text{-}actual}$). This is an indicator of the height of the cool, dry layer based on the MIST project.

e. The change in θ_e between the maximum θ_e in the lowest 150mb and $Min\,\theta_{e\text{-}actual}$ (K) ($\Delta\theta_{e\text{-}actual}$). This is the method used to compute $\Delta\theta_e$ in the MIST project (Atkins and Wakimoto 1991).

Parameters for a stratified random sample of 50 microburst producing thunderstorm days and 50 non-microburst producing thunderstorm days were used to build (or train) the index. Equal samples of microburst and non-microburst producing thunderstorm days were used since the statistical software package used in this thesis (S-

Plus 2000) performs best using equal samples from each group. The remaining 23 microburst producing thunderstorm days and a random sample of 39 non-microburst producing thunderstorm days were used to verify the new index. Since using 13 parameters is cumbersome for an index, a method was developed to determine which parameters were most important for microburst development.

A Pearson correlation coefficient (r) table (Appendix F), showing the r-values for each parameter as they relate to microburst occurrence and as they relate to each other, was developed using Statistix© for Windows©. The parameters that had the highest correlation to microburst occurrence and the least inter-correlation were used to build the index. They were $\Delta\theta_{e\text{-}actual}$, $P_{min\theta e\text{-}actual}$, and Γ. A discriminant analysis input table (matrix) was build using these parameters.

4.9.2 Building the Discriminant Analysis Input Table

A discriminant analysis input table is a tool for organizing the parameters that will be used to develop the discriminant function (Kachigan 1991). Table 7 is a generic discriminant analysis input table. Column 1 contains the objects that will be discriminated; for this thesis, it contains the days for which the predictor variables were measured. Column 2 indicates the group in which the object belongs. A 1 indicates a microburst producing thunderstorm day and a 0 indicates a non-microburst producing thunderstorm day. Columns 3, 4, and 5 are the predictor variables; they are equivalent to the transpose of matrix **X** in equation (17).

Object	Group	Predictor 1	Predictor 2	Predictor 3
Day 1	1	x_{11}	x_{12}	x_{13}
Day 2	1	x_{21}	x_{22}	x_{23}
Day 3	1	x_{31}	x_{32}	x_{33}
Day 4	1	x_{41}	x_{42}	x_{43}
Day 5	0	x_{51}	x_{52}	x_{53}
Day 6	0	x_{61}	x_{62}	x_{63}
Day 7	0	x_{71}	x_{72}	x_{73}
Day 8	0	x_{81}	x_{82}	x_{83}
Day 9	0	x_{91}	x_{92}	x_{93}

Table 7. Generic Discriminant Analysis Input Table (After Kachigan 1991).

Appendix G is the discriminant analysis input table for the 100 thunderstorm days used to train the discriminant function. Appendix H is the discriminant analysis input table for the 62 thunderstorm days used to verify the index.

4.9.3 Determining the Discriminant Weights

In 1936, Fisher developed a method for determining the discriminant weights based on the assumption that the variance-covariance matrices for each of the two groups have a common value (Dillon and Goldstein 1984). This common value is approximated by using the sample pooled variance-covariance matrix defined by the equation

$$\mathbf{S}_{\text{pooled}} = \frac{(n_1 - 1)[\mathbf{S}_1] + (n_2 - 1)[\mathbf{S}_2]}{(n_1 + n_2 - 1)} \tag{18}$$

where

$\mathbf{S}_{\text{pooled}}$ is the sample pooled variance-covariance matrix

$\mathbf{S}_1$ is the variance-covariance matrix for the predictor variables associated with group 1

$\mathbf{S}_2$ is the variance-covariance matrix for the predictor variables associated with group 2

n_1 is the number of objects measured in group 1, and

n_2 is the number of objects measured in group 2

The following equation is used to objectively determine the discriminant weights based on samples from each of the two groups.

$$\mathbf{b} = \mathbf{S}_{pooled}^{-1}(\bar{\mathbf{x}}_1 - \bar{\mathbf{x}}_2) \tag{19}$$

where

b is a vector of discriminant weights

$\mathbf{S}_{pooled}^{-1}$ is the inverse of the sample pooled variance-covariance matrix

$\bar{\mathbf{x}}_1$ is a vector of means of each predictor variable in group 1

$\bar{\mathbf{x}}_2$ is a vector of means of each predictor variable in group 2

S-Plus® 2000 was used to compute the sample pooled variance-covariance matrix and the group mean vectors for the stratified random sample of 100 thunderstorm days in Appendix G. A Mathcad template (Appendix I) was used to compute the discriminant weights based on the S-Plus® 2000 output.

4.9.4 Computing Discriminant Scores and Determining the Cutoff

A Mathcad template (Appendix I) was used to compute the discriminant scores for each group in the training sample in Appendix G using equation (17). The cutoff score was computed by the equation

$$Y_{cutoff} = \mathbf{b}' \frac{\bar{\mathbf{x}}_1 + \bar{\mathbf{x}}_2}{2} \tag{20}$$

where $\mathbf{b}'$, $\bar{\mathbf{x}}_1$, and $\bar{\mathbf{x}}_2$ are defined above. Equation (18) is valid only when the sample sizes of group 1 and group 2 are the same (Dillon and Goldstein 1984). Future observations of Y can be grouped based on Y_{cutoff} according to the rule

Y belongs to group 1 if it is greater than or equal to Y_{cutoff}

Y belongs to group 2 if it is less than Y_{cutoff}

4.9.5 Developing and Evaluating Confusion Matrix

A confusion matrix is a type of contingency table used to evaluate a discriminant function's ability to properly categorize objects or events. Table 8 is a generic confusion matrix for thunderstorm classification (microburst producing or non-microburst producing). Cells *a* and *d* indicate the number of correctly categorized thunderstorms. Cells *b* and *c* indicate the number of incorrectly categorized thunderstorms. Confusion matrices can be produced for the training data or for verification data (Dillon and Goldstein 1984). If the discriminant function is used to forecast events, the confusion matrix is the same as a contingency table for forecast verification.

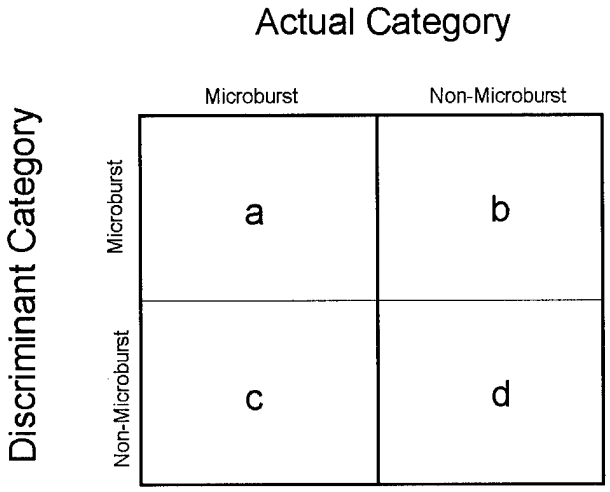

Table 8. Generic Confusion Matrix for Thunderstorm Category (Microburst Producing and Non-Microburst Producing).

4.9.6 Comparing Performance of the Discriminant Function (New Index) to MDPI

Once the discriminant weights and the cutoff score have been computed equation (17) takes the form of a new index similar to MDPI. Future measures of the predictor variables can be used to compute a discriminant score (Y) that is categorized as either a microburst producing thunderstorm day or a non-microburst producing thunderstorm day based on the cutoff score (Y_{cutoff}). Discriminant scores and MDPI values were computed using a stratified random sample of 62 thunderstorm days (23 that produced microbursts and 39 that did not) to compare the performance of the two indices. None of the validation thunderstorm days were used to train the discriminant function. Two contingency tables were produced: one containing the absolute frequencies, or counts, of forecast and observed microbursts based on the discriminant cutoff (Y_{cutoff}); the other containing the absolute frequencies based on MDPI. The indices were compared using POD, FAR, HR, TS, HSS and χ^2. Skill scores for POD, FAR, HR, and TS with MDPI as the reference forecast were also computed. Skill scores (SS) are interpreted as a percentage improvement over a reference forecast. They are computed with the following equation:

$$SS_{ref} = \frac{A - A_{ref}}{A_{perf} - A_{ref}} \times 100\% \qquad (21)$$

where

SS_{ref} is the skill score of a forecast technique with respect to some reference forecast technique

A is the accuracy score for the set of forecasts associated with the forecast technique being evaluated

A_{ref} is the accuracy score for a set of reference forecasts, and

A_{perf} is the accuracy score that would be achieved by a set of perfect forecasts.

5. Results and Conclusions

5.1 Introduction

This chapter summarizes the results and conclusions of this thesis using the methods described in Chapter 4. The last section lists opportunities for future research.

5.2 Fitting a Weibull Distribution to the KSC Microburst Climatology

The program Crystal Ball© was used to determine the Weibull shape and scale parameters that best fit the gust speed distribution of the 282 microbursts identified by Sanger (1999) in his KSC microburst climatology. The shape parameter (α) was 1.6263 and the scale parameter (β) was 16.88. Figure 11 shows a histogram of microburst gust speed with a rough distribution curve overlay. Figure 12 shows the fitted Weibull distribution based on the shape and scale parameters computed by Crystal Ball. Both figures were computed using Mathcad©. The curve in Figure 12 was integrated for each of the 45WS convective wind warning critical thresholds yielding the probability of having winds greater than 35 knots, 50 knots, and 60 knots should a microburst occur. All computations were done using Mathcad©. The resulting probabilities are

a. The probability of winds greater than 35 knots given microburst occurrence is .44
b. The probability of winds greater than 50 knots given microburst occurrence is .08
c. The probability of winds greater than 60 knots given microburst occurrence is .02

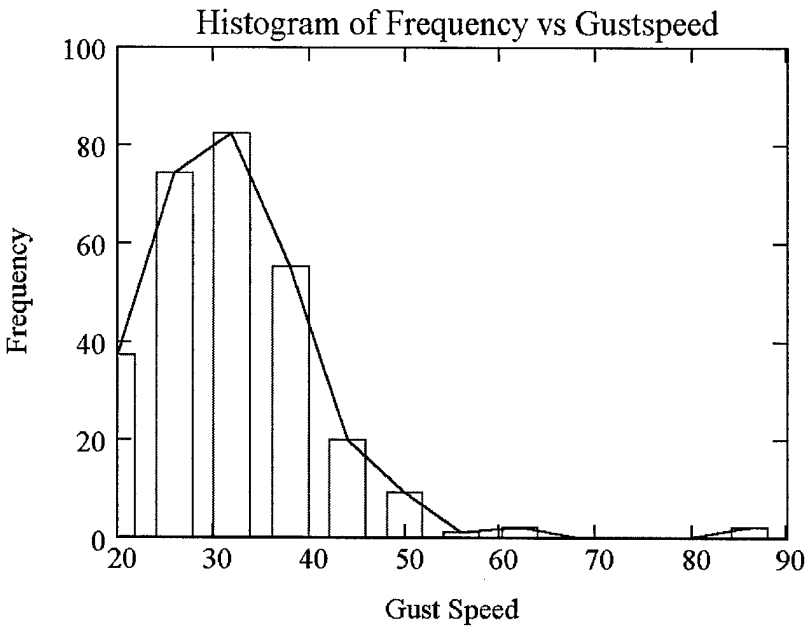

Figure 11. Histogram of Microburst Gust Speeds Identified by Sanger (1999) With Rough Distribution Curve Overlay.

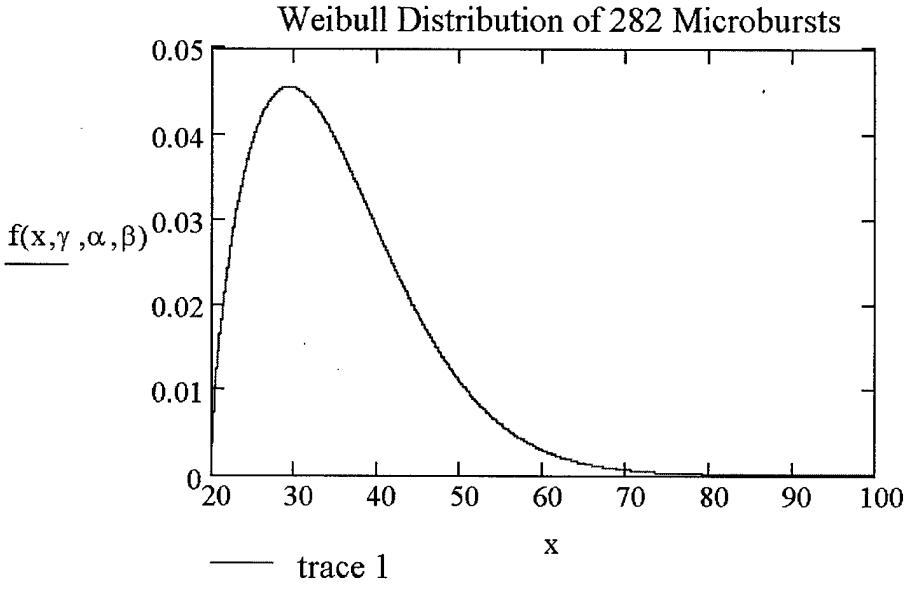

Figure 12. Weibull Distribution of 282 Microbursts Identified by Sanger.

5.3 Evaluation of MDPI

MDPI was computed for 73 microburst producing thunderstorm days and 167 non-microburst producing thunderstorm days using the procedure described in Chapter 3. Table 9 shows the 2 X 2 forecast verification contingency table for this data. The following accuracy and skill scores were computed using procedures described in Chapter 4.

Probability of Detection (POD) = 65%

False Alarm Rate (FAR) = 65%

Hit Rate (HR) = 51%

Threat Score (TS) = 29%

Heidke Skill Score (HSS) = 8%

Chi-Square (χ^2) = 2.12

P-value = .145

MDPI Evaluation

Forecast \ Observed	Yes	No
Yes	48	93
No	25	74

Table 9. 2 X 2 Forecast Verification Contingency Table For MDPI

Overall MDPI did not perform particularly well. A χ^2 test was used to assess the validity of the index. The null hypothesis was that the "hits" and "misses" produced by

MDPI are no better than those that would be assigned by a random selection process; the researcher's hypothesis was that the "hits" and "misses" produced by MDPI are better than those that would be generated by a random selection process. A χ^2 value of 2.706 or greater is required to reject the null for a significance level (α) of 0.1. The χ^2 of 2.12 indicates that the cell values produced by MDPI are not significantly better than those produced by random chance (the null is not rejected). Although the contingency table failed the χ^2 test, the POD, FAR, HR, TS and HSS were computed since these are the measures used to evaluate MDPI in previous studies. The POD indicates that 65% of the microbursts would have been identified using MDPI, however, the high FAR indicates that 65% of the forecast "microbursts" would fail to materialize. This high FAR is unacceptable. The HR of 51% shows that using MDPI to determine if a microburst will occur is only slightly better than flipping a coin. The HSS, which compares MDPI to random guessing, indicates that MDPI only beats random guessing by 8%.

The MDPI critical threshold (CT) was evaluated using a scatterplot of $\Delta\theta_e$ versus microburst occurrence (Figure 13). The large overlap of the two $\Delta\theta_e$ "populations" indicates that the current CT of 30K is as good as any other value depending on the level of acceptable error determined by the user.

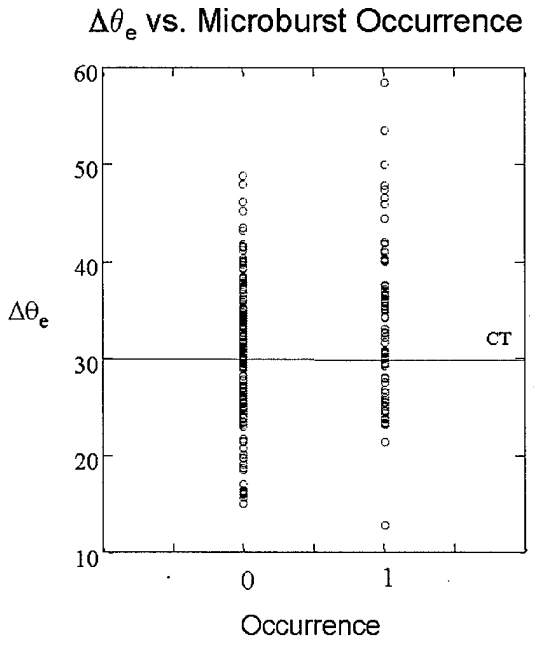

Figure 13. Scatterplot of $\Delta\theta_e$ vs Microburst Occurrence. A 0 indicates a non-microburst producing thunderstorm day and a 1 indicates a microburst producing thunderstorm day. The line marked CT is the MDPI critical threshold.

5.4 Evaluation of WINDEX

The Pearson correlation coefficient (r) was used to evaluate the degree of linear association between the maximum gust speeds predicted by WINDEX and the observed microburst gust speeds identified by Sanger (1999). Statistics® for Windows was used to compute r. The r-value was 0.24 (p-value 0.29) indicating very little correlation between WINDEX and the observed gust speeds. This result is consistent with r values computed in previous WINDEX studies (Roeder 1999).

A scatterplot of observed maximum gust speed versus WINDEX (Figure 14) was used to visually determine the degree of linear correlation and to see if a non-linear relationship exists. It is clear from the plot that no discernable linear or non-linear relationship exists between WINDEX and the observed microburst gust speed.

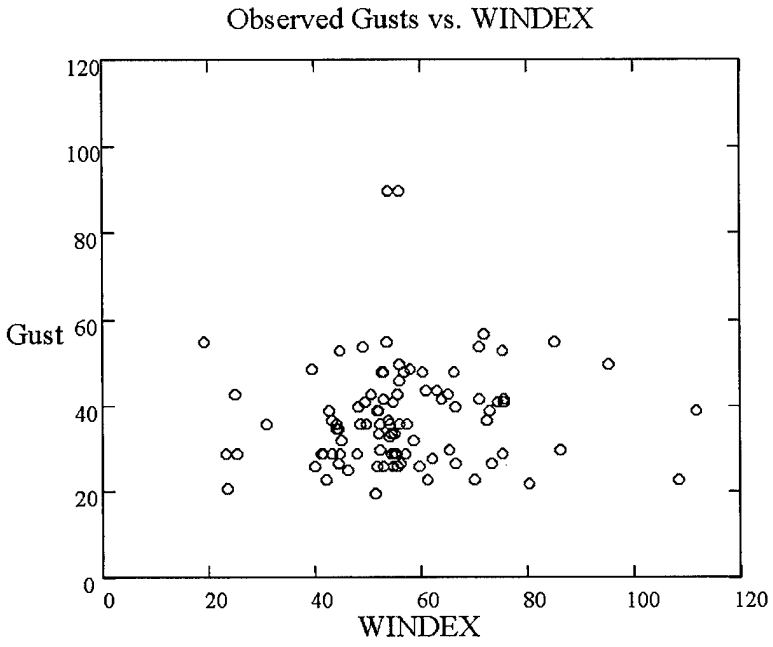

Figure 14. Scatterplot of Observed Microburst Gust Speed vs. WINDEX. It is clear from this plot that no discernable linear or non-linear relationship exists between WINDEX and the observed microburst gust speed.

5.5 New Index for Assessing Wet-Microburst Potential

A stratified sample of 50 microburst producing thunderstorm days and 50 non-microburst producing thunderstorm days was used to develop a new microburst potential index by way of discriminant analysis. The new index is

$$\text{New Microburst Index} = \frac{b_1(Maximum\,\theta_e - Minimum\,\theta_e) + b_2(P_{\min\theta_e}) + b_3(\Gamma)}{Y_{cutoff}} \qquad (21)$$

where

b_1, b_2, and b_3 are the discriminant weights 0.055 K^{-1}, -0.007876 mb^{-1}, and 0.966 km $°C^{-1}$ respectively

Y_{cutoff} is the discriminant cutoff 3.231

Maximum θ_e is the maximum value of θ_e in the lowest 150 mb of the sounding (K)

Minimum θ_e is the minimum value of θ_e in the entire sounding (K)

$P_{min\theta e}$ is the pressure level corresponding to *Minimum* θ_e (mb), and

Γ is the environmental lapse rate from the surface to the height of the melting level (°C km^{-1}).

New index values of 1 or greater indicate a strong potential for microburst development should a thunderstorm occur. New index values of less than 1 indicate a low potential for microburst development should a thunderstorm occur. This follows the same convention as MDPI.

Table 10 shows the confusion matrix for the 100 thunderstorm days used to train the index. Overall, the discriminant function classified 69% of the thunderstorm days correctly. The classification error rate was 31%. A χ^2 test was performed on the confusion matrix to determine if the classification procedure, defined by the discriminant function and cutoff, is statistically significant based on the training data set. The χ^2 of 14.49 and resulting *p*-value of 0.0001 imply that the procedure is statistically significant.

New Index Confusion Matrix

Discriminant Category	Actual Category: Microburst	Actual Category: Non-Microburst
Microburst	33	14
Non-Microburst	17	36

Table 10. New Index Confusion Matrix

A stratified random sample of 62 thunderstorm days (23 microburst producing and 39 non-microburst producing) was used to compare the performance of the new index to MDPI. None of the 62 verification thunderstorm days were used to build the new index. Table 11 shows the 2 X 2 forecast verification contingency table for MDPI based on the 62 thunderstorm day sample.

MDPI Verification

Forecast \ Observed	Yes	No
Yes	16	24
No	7	15

Table 11. 2 X 2 Forecast Verification Contingency Table for MDPI. This table is based on a stratified random sample of 62 thunderstorm days.

The following accuracy and skill scores were computed from Table 11.

POD = 69%

FAR = 60%

HR = 50%

TS =34%

HSS = 7%

$\chi^2 = .41$

P-value = .522

Overall MDPI performed about the same as the evaluation presented in section 5.3. Again a χ^2 test was used to assess the validity of the index. The null hypothesis was that the "hits" and "misses" produced by MDPI are no better than those that would be

generated by a random selection process; the researcher's hypothesis was that the "hits" and "misses" produced by MDPI are better than those that would be generated by a random selection process. Once again, the contingency table did not pass a χ^2 test for a significance level of 0.1 suggesting that the MDPI shows little merit. The *p*-value of .522 suggests that the χ^2 value of 0.14 would be attained 52.2% of the time as a result of a random selection process. Although the MDPI did not pass the χ^2 test, POD, FAR, HR, TS, and HSS were computed for comparative purposes. The 2 X 2 forecast verification contingency table for the new index is presented in Table 12.

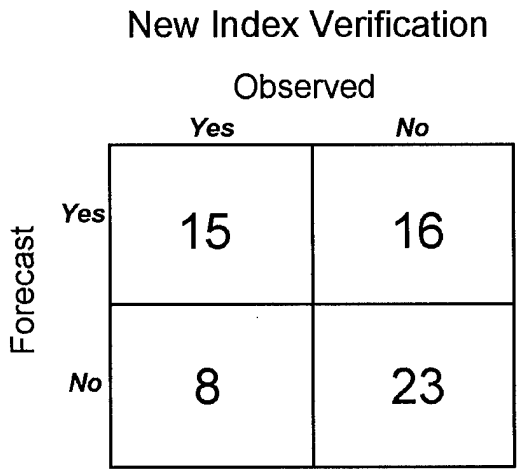

Table 12. 2 X 2 Forecast Verification Contingency Table for the New Index. This table is based on a random sample of 62 thunderstorm days.

The following accuracy and skill scores were computed from Table 12.

POD = 65%	HSS = 23%
FAR = 51%	$\chi^2 = 3.39$
HR = 61%	*P*-value = .066
TS = 38%	

The new index outperformed MDPI in almost all accuracy and skill scores. A χ^2 test was used to assess the validity of the new index. The null hypothesis was that the "hits" and "misses" produced by new index are no better than those that would be generated by a random selection process; the researcher's hypothesis was that the "hits" and "misses" produced by the new index are better than those that would be generated by a random selection process. The new index passed the χ^2 test for a significance level of 0.1 (the null was rejected). The *p*-value of 0.066 suggests that the χ^2 value of 3.39 would be attained only 6.6% of the time as a result of a random selection process. This implies a significant improvement over the MDPI which reported a *p*-value of 0.522 for the same sample.

As per equation 21, skill scores for the new index were computed using the POD, FAR, HR, and TS for MDPI as reference accuracy tests. The new index performed 13% worse than MDPI with respect to POD, 15% better than MDPI with respect to FAR, 22% better than MDPI with respect to HR, and 6% better than MDPI with respect to TS. The HSS shows that the new index beat random guessing by 23%. This is a marked improvement over MDPI which only beat random guessing by 7%. Table 13 compares the new index performance to that of MDPI.

	MDPI	New Index	Skill Score
POD	69%	65%	-13%
FAR	60%	51%	15%
HR	50%	61%	22%
TS	34%	38%	6%
HSS	7%	23%	N/A
χ^2	.41	3.39	N/A
P-Value	.522	.066	N/A

Table 13. MDPI and New Index Performance Comparison. Skill scores were computed using MDPI as the reference forecast.

5.6 Conclusion

Overall neither the MDPI nor the WINDEX performed particularly well. Neither index should be used operationally at the KSC/CCAS. The MDPI showed very little improvement over random guessing (HSS = 7%) and did not pass a χ^2 test for goodness of fit in either evaluation. The WINDEX showed very little correlation to observed maximum microburst gust speed (r = .24). Additionally, there was no discernable linear or non-linear relationship between WINDEX and observed maximum microburst gust speed. The Weibull distribution developed in this thesis is a good climatological starting point for assessing potential microburst gust speed.

A new index for predicting microburst potential was developed by way of discriminant analysis. Although the new index outperformed MDPI, its performance was, by no means, stellar. The new index did pass a χ^2 test for goodness of fit but showed only marginal improvement over random guessing (HSS = 23% and p-value

.066). Further refinement of the new index is needed to make it a more useful operational forecasting tool.

5.7 Opportunities for Future Research

There are five recommendations for future reasearch. They are

1) Add 1999 and 2000 microbursts to Sanger's (1999) KSC microburst climatology and evaluate the new index using an expanded data set

2) Redefine Γ as the environmental lapse rate from the surface to the height of the minimum θ_e aloft and re-evaluate the new index

3) Evaluate T1, T2, and Snyder methods for forecasting microburst gust speed at KSC/CCAS (found in AFWA TN-98/002 *Meteorological Techniques*)

4) Evaluate RAOB microburst prediction techniques used by the National Weather Service Office, Jackson, Mississippi for applicability at the KSC/CCAS. They include using Convective Available Potential Energy (CAPE), Vertical Totals (VT), and Wet Bulb Zero Height (WBZ) to assess microburst gust speed.

5) Evaluate the possibility of downward advection of momentum as a possible cause for microbursts at the KSC.

Appendix A: Microbursts Identified by Sanger (1999)

Year	Day	Time	Tower	Height	Direction	Speed	Gust
1995	11-May	2045	819	54	300	15	36
1995	11-May	2120	415	54	303	13	29
1995	11-May	2130	3131	162	344	28	40
1995	11-May	2215	300	54	325	21	41
1995	20-May	0500	9001	54	284	14	30
1995	20-May	0950	513	30	273	15	27
1995	20-May	0955	1007	54	278	18	29
1995	20-May	1000	394	60	262	21	36
1995	23-May	2020	2008	54	79	16	32
1995	5-Jun	1700	300	54	240	22	41
1995	10-Jun	2005	2202	54	326	25	44
1995	12-Jun	1645	1	54	261	21	39
1995	12-Jun	1700	393	60	257	16	30
1995	12-Jun	1700	398	60	257	16	35
1995	12-Jun	1850	2016	54	295	13	23
1995	12-Jun	1920	421	54	272	39	50
1995	12-Jun	2010	509	12	263	8	22
1995	12-Jun	2340	303	54	252	11	20
1995	12-Jun	2345	36	90	249	15	32
1995	18-Jun	1825	1000	54	39	13	26
1995	25-Jun	1950	511	30	196	15	41
1995	25-Jun	2005	412	54	172	11	21
1995	25-Jun	2015	1000	54	230	19	32
1995	26-Jun	2025	819	54	290	15	32
1995	26-Jun	2040	9001	54	259	14	34
1995	26-Jun	2050	403	54	262	12	37
1995	10-Jul	1840	412	54	299	13	27
1995	10-Jul	1850	394	60	318	19	36
1995	10-Jul	1850	398	60	303	25	46
1995	10-Jul	1925	506	54	171	14	36
1995	10-Jul	1930	1	54	231	13	30
1995	10-Jul	1935	3	54	256	15	30
1995	10-Jul	1935	61	162	319	13	28
1995	10-Jul	1935	108	12	147	2	21
1995	10-Jul	2125	2008	54	234	7	25
1995	10-Jul	2140	3131	54	302	13	27
1995	10-Jul	2210	509	12	328	15	34
1995	10-Jul	2230	1007	54	199	39	63
1995	13-Jul	1745	1612	54	250	15	28
1995	17-Jul	1750	398	60	239	3	21
1995	20-Jul	1820	805	54	105	15	32
1995	20-Jul	1855	3	54	263	19	32
1995	21-Jul	2000	1007	54	274	15	27
1995	21-Jul	2035	1	54	295	14	36

Year	Day	Time	Tower	Height	Direction	Speed	Gust
1995	21-Jul	2100	1101	162	206	21	39
1995	24-Jul	2035	513	30	234	13	27
1995	27-Jul	1555	403	12	168	12	23
1995	28-Jul	2145	397	60	109	16	37
1995	28-Jul	2145	398	60	109	18	40
1995	29-Jul	0930	311	54	162	15	29
1995	29-Jul	0935	412	54	134	13	29
1995	30-Jul	2050	397	60	66	18	29
1995	1-Aug	1520	819	54	72	9	25
1995	23-Aug	1615	61	54	101	16	30
1995	23-Aug	2235	61	54	109	22	39
1995	24-Aug	0600	1101	54	145	23	43
1995	24-Aug	0735	803	54	129	15	37
1995	24-Aug	0750	506	54	149	22	40
1995	24-Aug	0755	3131	54	150	23	49
1995	24-Aug	0830	108	12	162	7	27
1995	24-Aug	0840	511	30	140	18	36
1995	24-Aug	1100	1101	162	149	34	50
1995	24-Aug	1420	19	54	146	36	55
1995	24-Aug	1450	412	54	145	20	39
1995	26-Aug	2145	108	54	231	16	26
1995	27-Aug	1840	303	54	257	8	22
1995	27-Aug	2030	397	60	250	20	34
1995	31-Aug	0755	513	30	111	11	23
1995	12-Sep	1540	393	60	194	6	22
1995	13-Sep	1425	511	30	126	12	26
1995	25-Sep	0305	403	12	222	9	30
1995	26-Sep	0435	3131	162	182	13	32
1995	28-Sep	0025	513	30	169	16	34
1995	28-Sep	0200	1	54	60	25	42
1996	28-May	1950	40	54	153	4	43
1996	28-May	1950	61	204	289	13	37
1996	28-May	1950	311	54	15	16	39
1996	28-May	1950	3131	12	341	12	27
1996	28-May	1955	394	60	19	15	32
1996	28-May	2010	108	12	1	8	27
1996	31-May	0130	1	54	220	18	42
1996	31-May	0130	61	204	246	34	53
1996	31-May	0135	3	54	233	34	48
1996	9-Jun	1925	714	54	216	11	25
1996	9-Jun	2230	509	54	212	20	37
1996	19-Jun	2115	36	90	291	20	41
1996	20-Jun	1905	512	30	202	15	26
1996	20-Jun	1910	509	54	261	22	48
1996	26-Jun	1910	513	30	206	14	48
1996	27-Jun	2235	393	60	349	9	29

Year	Day	Time	Tower	Height	Direction	Speed	Gust
1996	4-Jul	1825	415	54	238	15	36
1996	4-Jul	1830	61	12	235	11	29
1996	4-Jul	1830	112	54	248	25	40
1996	4-Jul	1830	397	60	234	26	44
1996	5-Jul	2025	1101	162	156	14	25
1996	5-Jul	2035	311	54	161	8	20
1996	5-Jul	2115	1101	204	139	20	36
1996	5-Jul	2135	803	54	172	21	40
1996	6-Jul	1940	803	12	223	6	20
1996	6-Jul	1945	506	54	206	14	30
1996	6-Jul	2140	512	30	200	15	26
1996	6-Jul	2145	394	60	258	16	33
1996	6-Jul	2145	397	60	209	16	32
1996	6-Jul	2200	512	30	329	12	32
1996	11-Jul	2000	805	54	325	15	27
1996	11-Jul	2115	61	204	315	15	27
1996	23-Jul	2135	9001	54	269	9	29
1996	24-Jul	1930	393	60	265	20	44
1996	24-Jul	2055	1	54	258	13	30
1996	24-Jul	2055	403	54	253	13	23
1996	24-Jul	2100	805	54	194	11	32
1996	1-Aug	1745	1612	54	174	13	22
1996	1-Aug	1825	311	54	264	19	34
1996	1-Aug	1825	412	12	175	12	29
1996	3-Aug	1935	3131	204	248	16	33
1996	11-Aug	1730	512	30	224	16	90
1996	11-Aug	1735	3131	12	259	9	23
1996	13-Aug	1830	513	30	357	13	27
1996	15-Aug	2015	714	54	250	15	43
1996	15-Aug	2015	1204	54	323	15	39
1996	15-Aug	2025	61	204	295	22	34
1996	15-Aug	2025	1204	54	69	14	36
1996	15-Aug	2030	513	30	164	12	90
1996	15-Aug	2035	61	162	265	22	43
1996	19-Aug	2250	311	54	106	15	27
1996	19-Aug	2300	394	60	66	21	29
1996	20-Aug	0915	61	54	85	13	25
1996	20-Aug	1630	1605	54	84	15	35
1996	20-Aug	2100	421	54	68	15	29
1996	2-Sep	1715	1204	54	260	9	22
1996	2-Sep	1745	311	54	197	11	25
1996	2-Sep	1750	418	54	118	12	25
1996	2-Sep	1755	397	60	182	16	48
1996	2-Sep	1755	398	60	211	18	49
1996	6-Sep	0025	394	60	181	20	30
1996	7-Sep	0020	3131	54	263	8	29

Year	Days	Time	Tower	Height	Direction	Speed	Gust
1996	10-Sep	0710	41	54	321	3	20
1996	10-Sep	1245	1204	54	102	13	43
1996	10-Sep	1325	1204	54	92	11	39
1996	11-Sep	1635	394	60	276	14	29
1996	11-Sep	2005	1204	54	236	8	35
1996	17-Sep	1725	506	54	248	13	29
1996	17-Sep	1840	394	60	221	13	23
1996	17-Sep	2340	511	30	279	18	35
1996	18-Sep	2050	300	54	310	15	29
1997	3-May	1815	805	54	201	9	26
1997	3-May	1955	61	204	196	21	40
1997	3-May	2010	61	204	200	15	35
1997	3-May	2015	397	60	198	19	36
1997	3-May	2015	3131	295	194	27	37
1997	3-May	2020	41	54	206	14	35
1997	3-May	2020	1101	162	230	18	36
1997	3-May	2025	421	54	225	39	64
1997	3-May	2030	22	54	219	25	42
1997	28-May	0105	803	54	19	8	36
1997	28-May	0115	803	54	20	3	30
1997	28-May	1525	3	54	56	22	36
1997	31-May	1900	1012	54	182	8	25
1997	31-May	2205	3	12	259	11	22
1997	31-May	2205	112	54	223	18	39
1997	1-Jun	1750	509	54	215	22	55
1997	1-Jun	1755	415	54	268	12	25
1997	1-Jun	1805	512	30	233	19	41
1997	1-Jun	1825	403	54	264	28	42
1997	2-Jun	1520	3131	12	293	7	20
1997	2-Jun	2115	36	90	298	15	29
1997	12-Jun	1910	511	30	109	15	29
1997	12-Jun	2020	403	12	156	11	22
1997	12-Jun	2025	1	54	141	18	34
1997	12-Jun	2105	805	54	339	9	27
1997	14-Jun	1710	61	54	201	15	36
1997	14-Jun	1710	108	12	199	6	25
1997	14-Jun	1730	61	204	230	21	39
1997	14-Jun	1745	513	30	221	20	42
1997	17-Jun	1745	61	162	294	28	48
1997	19-Jun	2015	512	30	34	15	27
1997	19-Jun	2025	394	60	7	21	43
1997	19-Jun	2045	412	54	130	15	39
1997	19-Jun	2100	1000	54	33	18	28
1997	19-Jun	2110	3	54	332	22	48
1997	24-Jun	1730	2016	54	43	11	22
1997	27-Jun	1715	393	60	258	11	23

Year	Day	Time	Tower	Height	Direction	Speed	Gust
1997	29-Jun	2030	421	54	227	14	27
1997	1-Jul	0035	108	54	268	12	36
1997	1-Jul	2130	412	54	213	11	33
1997	1-Jul	2130	511	30	110	11	32
1997	5-Jul	1925	714	54	135	15	28
1997	5-Jul	1935	1012	54	195	12	30
1997	9-Jul	2110	805	54	328	15	39
1997	19-Jul	2045	300	54	288	20	36
1997	26-Jul	1835	1612	54	283	9	34
1997	26-Jul	1900	1012	54	274	16	49
1997	26-Jul	1925	714	54	322	11	46
1997	27-Jul	2020	393	60	317	23	37
1997	29-Jul	2130	421	54	154	22	43
1997	3-Aug	2105	41	54	239	19	36
1997	4-Aug	1905	393	60	281	22	48
1997	6-Aug	2225	819	54	309	8	20
1997	10-Aug	2005	19	54	298	34	50
1997	10-Aug	2005	805	12	315	5	28
1997	10-Aug	2025	509	54	188	18	33
1997	10-Aug	2125	61	162	273	15	34
1997	19-Aug	1805	1101	162	115	22	43
1997	19-Aug	1810	112	12	53	4	20
1997	19-Aug	1825	1500	54	247	8	25
1997	19-Aug	1835	311	12	209	7	20
1997	20-Aug	2150	513	30	326	23	43
1997	20-Aug	2155	3131	295	299	23	42
1997	23-Aug	2040	803	54	45	6	29
1997	1-Sep	1040	3	54	68	18	28
1997	1-Sep	1105	393	60	121	22	34
1997	1-Sep	1320	3	54	75	23	32
1997	1-Sep	1530	803	54	71	6	26
1997	3-Sep	2005	3131	162	289	13	29
1997	23-Sep	0750	506	54	212	15	36
1997	25-Sep	2025	1000	54	244	16	34
1997	26-Sep	1755	1612	54	205	12	27
1997	26-Sep	1820	803	54	220	16	29
1997	26-Sep	1835	61	204	194	18	36
1997	26-Sep	1840	3131	12	173	9	28
1997	26-Sep	1845	397	60	215	18	34
1998	4-May	1900	112	54	293	14	32
1998	4-May	1950	1000	54	283	19	41
1998	5-May	1745	1007	54	213	16	53
1998	7-Jun	1925	9001	54	336	18	47
1998	21-Jun	0105	418	54	227	22	43
1998	21-Jun	2130	300	54	309	19	35
1998	21-Jun	2140	300	54	337	11	39

Year	Day	Time	Tower	Height	Direction	Speed	Gust
1998	26-Jun	1830	1101	54	238	22	39
1998	26-Jun	1845	41	54	201	13	34
1998	6-Jul	1925	1612	54	75	32	55
1998	6-Jul	2005	1612	54	248	11	30
1998	7-Jul	1640	1007	54	231	16	29
1998	11-Jul	1825	300	54	292	14	26
1998	18-Jul	2215	511	30	248	18	33
1998	18-Jul	2215	512	30	224	28	44
1998	18-Jul	2215	513	30	192	25	43
1998	18-Jul	2250	819	54	225	13	36
1998	26-Jul	1930	819	54	221	12	29
1998	28-Jul	0220	1000	54	203	3	26
1998	28-Jul	0230	303	54	208	13	35
1998	28-Jul	0300	108	54	311	18	43
1998	28-Jul	0300	112	12	177	13	27
1998	28-Jul	0300	1101	162	188	36	57
1998	28-Jul	2105	421	54	8	16	29
1998	28-Jul	2120	421	54	340	18	34
1998	28-Jul	2135	418	54	308	18	39
1998	28-Jul	2145	714	12	21	11	32
1998	28-Jul	2150	112	54	353	11	33
1998	28-Jul	2150	398	60	336	20	35
1998	28-Jul	2150	1101	204	14	16	36
1998	28-Jul	2200	397	60	316	26	51
1998	28-Jul	2200	398	60	307	15	41
1998	28-Jul	2200	513	30	189	5	36
1998	28-Jul	2200	3131	295	354	29	44
1998	28-Jul	2225	1007	54	274	13	47
1998	29-Jul	1745	311	54	32	9	26
1998	5-Aug	1855	1000	54	7	21	42
1998	6-Aug	1750	805	54	135	15	32
1998	10-Aug	1935	714	54	259	8	28
1998	13-Aug	1955	421	54	7	22	41
1998	13-Aug	2015	714	54	13	21	40
1998	13-Aug	2045	3131	204	351	30	43
1998	14-Aug	1900	819	54	137	18	43
1998	14-Aug	1955	61	204	288	25	36
1998	14-Aug	2020	1000	54	73	16	32
1998	17-Aug	1645	311	54	114	12	26
1998	21-Aug	0615	3131	204	129	22	36
1998	22-Aug	0220	311	54	137	14	34
1998	22-Aug	0220	397	60	144	22	37
1998	22-Aug	0220	398	60	139	26	40
1998	31-Aug	1805	1007	54	13	21	39
1998	31-Aug	1815	714	54	251	18	35
1998	3-Sep	0030	300	54	135	15	30

Year	Day	Time	Tower	Height	Direction	Speed	Gust
1998	3-Sep	1815	9001	54	238	14	39
1998	3-Sep	1825	803	12	234	9	28
1998	3-Sep	1830	403	54	244	18	40
1998	3-Sep	1835	108	54	245	27	43
1998	3-Sep	1900	421	54	214	27	46
1998	7-Sep	2145	513	30	169	19	33
1998	24-Sep	1230	311	54	67	18	29
1998	25-Sep	2055	3	54	162	25	34

Appendix B: Sample WINDS Data

DAY	TIME	IDN	Z	DIR	SPD	GUS	DDEV	T	TD	RH
94121	0	1	6					76		
94121	0	1	12	113	6	9	16			
94121	0	1	54	123	12	13	7	76		
94121	0	3	6					78		
94121	0	3	12	99	11	13	6			
94121	0	3	54	108	13	13	7	77		
94121	0	6	6							
94121	0	6	12							
94121	0	6	54							
94121	0	6	162							
94121	0	6	204							
94121	0	108	6					75		
94121	0	108	12	100	3	7	25			
94121	0	108	54	111	8	11	11	73		
94121	0	110	6					76	70	79
94121	0	110	12	105	5	7	11			
94121	0	110	54	111	8	9	9	76	69	79
94121	0	110	162	101	10	11	6			
94121	0	110	204	103	11	12	5	76	69	78
94121	0	112	6					77		
94121	0	112	12	104	4	8	15			
94121	0	112	54	102	8	10	9	77		
94121	0	303	6					76		
94121	0	303	12	108	3	4	20			
94121	0	303	54	113	6	9	13	75		
94121	0	311	6					76		
94121	0	311	12	119	5	8	16			
94121	0	311	54	105	8	10	11	74		
94121	0	313	6					76	64	68
94121	0	313	12	127	5	8	11			
94121	0	313	54	108	7	10	10	77	66	71
94121	0	313	162	115	11	13	6			
94121	0	313	204	115	12	13	7	76	66	73
94121	0	313	295	120	13	14	7			
94121	0	313	394	112	13	14	7			
94121	0	313	492	109	14	14	6	75	66	73
94121	0	403	6					76		
94121	0	403	12	134	5	7	13			
94121	0	403	54	123	6	10	11	76		
94121	0	412	6					76		
94121	0	412	12	106	5	7	14			
94121	0	412	54	98	8	11	10	75		
94121	0	415	6					74		
94121	0	415	12	124	3	5	17			
94121	0	415	54	99	6	8	10	75		
94121	0	506	6					76		
94121	0	506	12	106	4	6	14			
94121	0	506	54	107	8	10	11	76		
94121	0	509	6					74		
94121	0	509	12	103	3	4	18			
94121	0	509	54	105	5	6	9	74		

Appendix C: Sample Upper-Air Sounding in Decoded Format

```
15 4 5 1998 1013 5 25.8 16.8 210 8
15 4 5 1998 1011 22 24.6 17.6 999 999
15 4 5 1998 1000 123 24.2 18.2 215 13
15 4 5 1998 992 193 23.8 18.8 999 999
15 4 5 1998 979.4 304 999 999 210 16
15 4 5 1998 969 396 22 18.1 999 999
15 4 5 1998 948 584 20.4 16.8 999 999
15 4 5 1998 945.2 609 999 999 210 18
15 4 5 1998 933 721 20.8 10.8 999 999
15 4 5 1998 926 786 21.4 3.4 999 999
15 4 5 1998 925 796 999 999 999 999
15 4 5 1998 913 907 20.6 8.6 999 999
15 4 5 1998 912.3 914 999 999 205 22
15 4 5 1998 880.7 1219 999 999 205 22
15 4 5 1998 850.2 1524 999 999 205 22
15 4 5 1998 850 1526 14.8 4.8 210 22
15 4 5 1998 837 1655 13.8 3.8 999 999
15 4 5 1998 819.8 1828 999 999 210 20
15 4 5 1998 790.3 2133 999 999 210 18
15 4 5 1998 785 2189 10.6 -4.4 999 999
15 4 5 1998 770 2349 9.8 -3.2 999 999
15 4 5 1998 761.7 2438 999 999 215 18
15 4 5 1998 733.8 2743 999 999 220 21
15 4 5 1998 710 3013 4.6 -5.4 999 999
15 4 5 1998 700 3138 3.8 -6.2 225 22
15 4 5 1998 655.9 3657 999 999 240 22
15 4 5 1998 632 3954 -3.5 -6.8 999 999
15 4 5 1998 612 4207 -4.5 -6.7 999 999
15 4 5 1998 607.3 4267 999 999 260 24
15 4 5 1998 603 4323 -4.9 -8.7 999 999
15 4 5 1998 590 4493 -6.3 -10.3 999 999
15 4 5 1998 561.5 4876 999 999 260 26
15 4 5 1998 550 5036 -10.7 -15.7 999 999
15 4 5 1998 524 5405 -14.1 -16.5 999 999
15 4 5 1998 518.6 5486 999 999 255 28
15 4 5 1998 500 5770 -16.1 -17.5 250 28
15 4 5 1998 490 5921 -17.5 -18.3 999 999
15 4 5 1998 478.6 6096 999 999 245 29
15 4 5 1998 463 6342 -19.9 -21.3 999 999
15 4 5 1998 453 6503 -21.1 -23 999 999
15 4 5 1998 442 6684 -22.1 -27.1 999 999
15 4 5 1998 430 6885 -23.7 -31.7 999 999
15 4 5 1998 419 7073 -25.3 -36.3 999 999
15 4 5 1998 400 7410 -28.1 -38.1 265 34
```

Appendix D: IDL Program for Data Interpolation, and Computing MDPI and WINDEX

```
pro parameters10m, fn

  ; This program will interpolate missing temp and dp data from upper-air soundings and
  ; compute MDPI, WINDEX and associated parameters. Data is read-in in the format:
  ;Time,Day,Month, Year,Press,Height,Temp,Dewpoint,Direction,Speed. All parameters
  ;are saved to an output file.

  ; Written By: Steven Dickerson
  ; Last updated: 2 Dec 1999

  ; Count the number of lines in the sounding

n = 0
s = ' '
close, 5
openr, 5, fn
while not (eof(5)) do begin
readf, 5, s
if (strlen(s) GT 5) then n = n+1
endwhile
point_lun, 5, 0

  ; Now read in the sounding data

data = fltarr(10,n)
readf, 5, data
close, 5

  ;********This identifies the variable associated with each column of the array*******

time = data[0,*]
day = data[1,*]
month = data[2,*]
year = data[3,*]
pres = data[4,*]
hgt = data[5,*]
temp = data[6,*]
dp = data[7,*]
dir = data[8,*]
spd = data[9,*]
;rh = data[10,*]

  ; This identifies where the missing values of temp are
```

```
blanks = Where(strpos(temp, '999.0') GE 0, bc)
nonblank = Where(strpos(temp, '999.0') LT 0, nbc)

for i = 0L, bc-1 do begin

  ; find obs before 999.0 with number

before = max(where(nonblank LT blanks(i)))
after = min(where(nonblank GT blanks(i)))

temp(blanks(i)) = temp(nonblank(before)) + ( (temp(nonblank(after))-
temp(nonblank(before))) * ( (hgt[blanks(i)] -
hgt[nonblank(before)])/(hgt[nonblank(after)]-hgt[nonblank(before)]) ) )

;weight=( (hgt[blanks(i)] - hgt[nonblank(before)])/(hgt[nonblank(after)]-
hgt[nonblank(before)]) )
;print,weight

endfor

; This identifies where the missing values of DP are

blank = Where(strpos(dp, '999.0') GE 0, bc)
nonblanks = Where(strpos(dp, '999.0') LT 0, nbc)

for i = 0L, bc-1 do begin

  ; find obs before 999.0 with number

before = max(where(nonblanks LT blank(i)))
after = min(where(nonblanks GT blank(i)))

dp(blank(i)) = dp(nonblanks(before)) + ( (dp(nonblanks(after))-dp(nonblanks(before))) *
( (hgt[blank(i)] - hgt[nonblanks(before)])/(hgt[nonblanks(after)]-hgt[nonblanks(before)])
) )

endfor

; ************* This section builds a  Theta-E profile of the Atms ****************

for i = 0, n-1 do begin

        ; compute the temperature at the Lifted Condensation Level
```

```
TLCL = dp(0) - (0.212+.001571*dp(0)-.000436*temp(0))*(temp(0)-dp(0))+273.16

        ; compute the mixing ratio

e = 6.112*exp((17.67*dp)/(dp+243.5))
r = .622*((e)/(pres-e))

  ; Now compute thetaE

k=.2854

thetaE = (temp+273.16)*((1000.0/pres)^(k*(1.0-(.28*r))))*exp(((3376/TLCL)-
2.54)*r*(1+(.81*r)))

endfor

; ********** This section computes the delta-ThetaE needed for MDPI **********

position_lowest_150mb = where(pres GE (max(pres)-150))
lowPres = pres(position_lowest_150mb)
maxThetaE = max(thetaE(position_lowest_150mb))
maxPres = lowPres(where(max(thetaE(position_lowest_150mb))))

;deltaThetaE=maxThetaE-min(thetaE)

;position_minPres = where(thetaE EQ min(thetaE))
;minPres = pres(position_minPres)

position_minPres = where(pres GE 500 and pres LE 650)   ; **********************
midlevel_Pres = pres(position_minPres)                                        *
midlevel_thetaE = thetaE(position_minPres)              ;*Compute using min at mid*
minThetaE = min(midlevel_thetaE)                        ; *      levels          *
minPres = pres(where(thetaE EQ min(midlevel_thetaE)))   ; **********************

deltaThetaE = maxThetaE - minThetaE

min_P_Total = pres(where(thetaE EQ min(thetaE)))
min_TH_Total = min(thetaE)
delta_Total = maxThetaE - min_TH_Total

; ********** This section computes the Vertical Totals **********
Pres850=where(pres EQ 850)
Pres500=where(pres EQ 500)
```

```
if ((min(Pres850)) AND (min(Pres500)) GT 0) then begin ; min statements needed to
change from array to scalar

VT = temp(where(pres EQ 850)) - temp(where(pres EQ 500))

endif else begin
VT = 9999 ; if 850 or 500 mb level is missing 9999 is reported at VT

endelse

; ********** This section computes the WINDEX parameters **********

;********** Find the Height of the Melting Level (Hm) in kilometers **********

position_below_zero = where(temp LE 0)
hgt_below_zero = hgt(position_below_zero)

Hm = hgt_below_zero(0)/1000


;********** Find the Mixing Ratio at the Melting Level (Qm) in g/kg **********

pres_below_zero = pres(position_below_zero)
pres_ML = pres_below_zero(0)

dp_below_zero = dp(position_below_zero)
dp_ML = dp_below_zero(0)

vaporpress = 6.112*exp((17.67*dp_ML)/(dp_ML+243.5))
Qm = (.622*((vaporpress)/(pres_ML-vaporpress)))*1000


;*** Find the Mean Mixing Ratio in the lowest 1km of the Atmosphere (QL) in g/kg ***

position_lowest_1km = where(hgt LE 1000)
dp_lowest_1km = dp(position_lowest_1km)
pres_lowest_1km = pres(position_lowest_1km)


for i=0, n-1 do begin

vaporpress = 6.112*exp((17.67*dp_lowest_1km)/(dp_lowest_1km+243.5))
mixingratio = (.622*((vaporpress)/(pres_lowest_1km-vaporpress)))*1000.0

number = n_elements(mixingratio)
```

```
QL = (mixingratio(0) + mixingratio(number-1))/2

endfor
;********************** Now compute Rq ********************************

Rq = QL/12

if (Rq GT 1) then Rq=1.0

;***** Now find the Mean Environmental Lapse Rate (gamma) in degrees C per 1km
*******

temp_LT_zero=temp(position_below_zero)
gamma = ((temp(0)-temp_LT_zero(0))/Hm)

;********************** Now Compute WINDEX (WI) ************************

WI = 5*(Hm*Rq*(gamma^2 - 30 +QL - 2*Qm))^.5

new_array = [time, day, month, year, pres, thetaE, hgt, temp, dp]

output = [maxPres, maxThetaE, minPres, minThetaE, min_P_Total, min_TH_Total,
deltaThetaE, delta_Total, VT, Hm, Qm, QL, Rq, gamma, WI]
print, output


openu, outfile, "parameters-micro-new.txt", /get_lun, /append
printf, outfile, fn
close, outfile
free_lun, outfile

openu, outfile, "parameters-micro-new.txt", /get_lun, /append, width = 300
printf, outfile, output
close, outfile
free_lun, outfile

end
```

Appendix E: MDPI and WINDEX Parameters

Legend

YR -- Year

MO -- Month

DY -- Day

OCR -- Occurrence or non-occurrence of microburst. A 1 indicates that this day is a microburst producing thunderstorm day; a 0 indicates that this is a non-microburst producing thunderstorm day

MaxPr -- The pressure level (mb) corresponding to the maximum θ_e recorded in the lowest 150 mb of the sounding

MaxThetE -- The maximum θ_e (K) recorded in the lowest 150 mb of the sounding

MinPr -- The pressure level (mb) corresponding to the minimum θ_e found between 650 and 500 mb

MinThetaE -- The minimum θ_e (K) found between 650 and 500 mb

MinPActu -- The pressure level (mb) corresponding to the minimum θ_e found at any level in the sounding

MinTActu -- The minimum θ_e (K) found at any level in the sounding

MDPI -- MaxThetE - MinThetaE

DeltaActua -- MaxThetE - MinTActu

Hm -- The height of the melting level (km)

Qm -- The mixing ratio at the height of the melting level ($g\ kg^{-1}$)

Ql -- The mixing ratio in the lowest 1 km of the atmosphere ($g\ kg^{-1}$)

gamma -- The environmental lapse ($°C\ km^{-1}$) rate from the surface to the height of the melting level

WI -- The computed WINDEX value

YR	MO	DY	OCR	MaxPr	MaxThetE	MinPr	MinThetaE	MinPActu	MinTActu	MDPI	DeltaActua	Hm	Qm	QI	gamma	WI
95	5	11	1	1014	354.491	641	319.236	723	317.631	35.255	36.8599	5.364	1.0349	16.126	6.3386	57.006
95	5	12	0	1012	348.825	614	322.318	614	322.318	26.507	26.5071	4.875	1.7927	13.803	6.3348	49.799
95	5	19	0	1013	359.291	567	321.21	706	314.459	38.081	44.8315	4.875	0.6539	18.101	6.6765	61.831
95	5	23	1	1017	351.57	611	320.793	700	319.631	30.776	31.9383	4.267	2.2909	15.19	6.5756	50.436
95	5	28	0	1019	348.17	615	322.935	804	316.765	25.235	31.4046	4.942	1.5119	14.997	5.6657	41.699
95	6	17	0	1020	343.436	613	318.824	676	315.823	24.612	27.6133	4.268	1.6508	14.119	6.7948	53.66
95	6	18	1	1017	348.423	650	320.262	697	318.583	28.161	29.8398	4.267	4.1909	14.219	7.1029	52.956
95	6	21	0	1013	349.029	610	332.793	466	329.035	16.236	19.9941	4.875	4.953	14.674	6.1868	39.872
95	6	23	0	1016	352.317	615	331.509	666	328.681	20.809	23.637	4.875	4.347	16.132	5.3575	27.356
95	6	24	0	1014	347.473	545	321.205	545	321.205	26.268	26.2678	4.378	5.4944	14.505	6.1672	35.555
95	6	25	1	1013	365.417	561	323.317	561	323.317	42.1	42.0995	4.581	6.0593	16.955	6.5488	45.052
95	6	26	1	1016	354.135	522	321.439	705	321.191	32.697	32.9438	4.418	5.9272	16.515	6.5641	44.274
95	6	28	0	1017	368.893	500	325.287	500	325.287	43.606	43.6061	4.815	4.6067	19.176	6.4382	50.771
95	6	30	0	1015	361.327	635	324.426	741	322.886	36.901	38.441	4.52	4.8095	15.849	6.8584	51.276
95	6	5	1	1009	357.457	506	331.928	703	330.213	25.53	27.2448	5.112	4.4631	17.544	5.6729	37.152
95	6	10	1	1017	355.244	614	324.559	614	324.559	30.685	30.6852	4.572	2.5625	15.408	6.7974	55.022
95	6	11	0	1016	356.948	586	319.706	721	312.272	37.242	44.6765	3.957	5.6164	15.403	7.5815	55.954
95	6	12	1	1012	359.455	627	323.84	627	323.84	35.614	35.6141	4.875	2.5623	16.468	6.7463	57.211
95	7	1	0	1015	357.551	603	321.714	603	321.714	35.837	35.8369	4.401	2.1529	15.979	6.5894	52.544
95	7	6	0	1020	351.104	500	327.019	852	320.721	24.085	30.383	4.869	3.9716	13.704	6.3668	44.54
95	7	8	0	1016	349.203	649	317.651	649	317.651	31.552	31.5515	5.889	0.8405	14.004	6.6225	62.085
95	7	11	0	1017	352.794	637	323.4	668	323.036	29.394	29.7585	4.124	3.9233	16.003	7.032	53.349
95	7	12	0	1015	352.395	588	323.158	491	323.078	29.236	29.3167	4.875	1.6079	16.583	5.8162	45.779
95	7	14	0	1018	352.977	517	323.501	517	323.501	29.476	29.476	4.537	3.2654	14.4	6.3919	46.087
95	7	17	1	1014	351.745	546	327.958	477	326.232	23.787	25.5138	4.404	5.9372	16.492	5.4496	21.799
95	7	24	1	1017	363.506	628	328.508	628	328.508	34.998	34.9978	4.676	5.2481	18.464	6.8435	53.844
95	7	25	0	1018	359.568	530	329.088	530	329.088	30.479	30.4794	4.643	6.0802	18.029	6.246	41.56
95	7	26	0	1018	353.536	649	334.503	700	332.729	19.033	20.8067	4.874	5.3967	15.748	5.9499	35.524
95	7	27	1	1016	364.991	500	335.598	700	330.509	29.394	34.4821	5.91	3.8831	17.615	6.2606	53.045
95	7	28	1	1017	360.991	615	320.829	615	320.829	40.162	40.1619	4.572	2.0381	17.392	6.6779	56.48
95	7	30	1	1018	360.217	585	319.847	585	319.847	40.37	40.3701	4.673	0.5431	18.088	6.2059	54.596
95	7	30	0	1018	360.217	585	319.847	585	319.847	40.37	40.3701	4.673	0.5431	18.088	6.2059	54.596
95	8	21	0	1015	365.236	615	332.694	615	332.694	32.542	32.5415	5.178	5.2077	19.175	5.9869	43.477

YR	MO	DY	OCR	MaxPr	MaxThetE	MinPr	MinThetaE	MinPActu	MinTActu	MDPI	DeltaActua	Hm	Qm	QI	gamma	WI
95	8	23	1	1011	362.096	545	337.683	545	337.683	24.413	24.4132	5.193	5.6465	17.653	5.5844	31.3
95	8	26	1	1013	361.419	543	335.866	463	332.586	25.553	28.8326	4.87	5.8155	17.231	5.9548	36.695
95	8	27	1	1014	353.264	603	325.745	603	325.745	27.52	27.5195	5.18	1.9308	14.828	5.7874	43.273
95	8	30	0	1011	367.383	500	327.931	500	327.931	39.452	39.4521	5.18	3.599	20.104	5.6854	44.411
95	8	1	1	1014	353.426	535	322.918	535	322.918	30.508	30.5078	4.564	2.8055	16.282	6.135	45.707
95	8	8	0	1017	357.397	649	319.566	693	316.182	37.831	41.2154	5.246	0.5302	16.307	5.9093	51.428
95	8	10	0	1012	358.065	587	320.877	587	320.877	37.188	37.1876	4.736	4.9439	16.526	6.1233	40.907
95	9	2	0	1009	369.043	630	320.942	630	320.942	48.101	48.1011	5.409	1.4792	19.619	5.9161	54.12
95	9	3	0	1015	352.365	612	320.399	690	316.617	31.966	35.7476	4.705	0.5478	14.812	6.3762	53.542
95	9	4	0	1017	351.695	567	321.459	567	321.459	30.235	30.2353	4.472	1.8401	15.393	6.4848	51.546
95	9	6	0	1014	349.864	601	326.315	601	326.315	23.549	23.5493	4.875	3.5729	15.535	6.2161	45.557
95	9	7	0	1012	351.695	610	332.851	752	330.734	18.844	20.9608	4.786	5.3776	14.958	6.4772	43.969
95	9	8	0	1011	357.13	634	330.621	634	330.621	26.509	26.5092	4.572	5.2824	17.181	6.4164	45.089
95	9	9	0	1013	356.964	576	325.98	576	325.98	30.984	30.9844	4.267	5.2196	15.574	7.0226	51.072
95	9	12	1	1019	364.471	571	330.208	571	330.208	34.264	34.2638	4.875	3.8597	18.497	6.3826	51.207
95	9	14	0	1020	354.391	538	327.002	538	327.002	27.389	27.3894	4.594	4.1368	16.418	6.5303	48.863
95	9	15	0	1020	357.191	538	326.722	728	326.275	30.469	30.9163	4.875	3.7232	14.419	6.3244	45.479
95	9	16	0	1018	352.638	574	324.718	574	324.718	27.921	27.9205	4.426	4.737	16.086	6.5522	46.502
95	9	18	0	1011	371.276	500	334.388	500	334.388	36.888	36.8882	5.55	4.0218	20.124	6.3063	55.061
95	9	23	0	1015	362.585	638	329.882	689	327.336	32.704	35.2491	5.193	3.8368	17.865	6.1621	48.56
95	9	24	0	1015	354.109	522	323.915	718	320.208	30.194	33.9017	4.875	2.8416	15.968	6.3231	49.699
95	9	27	0	1014	360.236	633	333.162	739	321.129	27.075	39.1073	4.875	5.0547	17.745	6.0922	42.4
95	9	28	0	1014	358.978	537	325.218	537	325.218	33.76	33.76	4.875	2.3079	18.284	5.9325	47.946
95	9	1	0	1011	362.529	534	329.037	534	329.037	33.492	33.4924	4.583	6.0697	18.357	6.3277	43.159
96	5	25	0	1017	359.734	597	317.968	597	317.968	41.766	41.7661	4.475	0.5322	18.383	6.4803	57.267
96	5	27	0	1015	357.722	585	323.667	486	323.573	34.055	34.1484	4.627	1.8811	16.815	6.4839	53.876
96	5	28	1	1015	356.48	616	320.266	678	319.286	36.214	37.194	4.622	1.5899	16.149	6.2744	50.803
96	5	30	0	1012	352.352	582	321.598	582	321.598	30.754	30.7538	4.635	2.2309	15.661	6.6881	54.815
96	6	16	0	1017	348.372	509	323.139	509	323.139	25.233	25.2333	4.791	3.6681	15.014	6.0528	41.407
96	6	19	1	1015	350.585	519	325.886	519	325.886	24.699	24.6991	4.067	6.123	14.577	7.1307	48.544
96	6	20	1	1015	356.89	566	328.894	666	327.726	27.996	29.1636	4.505	4.1298	15.579	5.9934	38.616
96	6	21	0	1015	355.579	560	327.275	560	327.275	28.303	28.3034	4.767	3.6489	16.677	6.7127	53.969
96	6	22	0	1015	362.387	649	329.189	649	329.189	33.199	33.1985	4.894	4.7829	17.646	6.2621	45.999

YR	MO	DY	OCR	MaxPr	MaxThetE	MinPr	MinThetaE	MinPActu	MinTActu	MDPI	DeltaActua	Hm	Qm	Ql	gamma	Wl
96	6	23	0	1016	361.159	598	323.041	598	323.041	38.118	38.1181	5.42	0.4481	17.37	6.0886	56.484
96	6	25	0	1016	369.48	589	320.546	589	320.546	48.934	48.9344	4.877	0.674	18.7	6.4678	59.652
96	6	26	1	1017	358.638	621	323.643	621	323.643	34.995	34.9947	4.414	3.2057	16.378	7.0229	56.851
96	6	28	0	1015	358.811	572	333.673	661	333.348	25.138	25.4626	4.806	4.6229	17.799	5.826	38.746
96	6	8	0	1016	359.901	539	322.035	733	321.058	37.866	38.8438	4.267	4.165	17.306	7.0528	55.348
96	6	9	1	1016	354.488	541	322.743	541	322.743	31.744	31.7443	4.386	2.533	14.208	6.6118	50.064
96	6	11	0	1017	355.951	567	324.208	567	324.208	31.742	31.7424	4.262	5.0068	14.178	6.5697	42.965
96	6	12	0	1018	351.414	613	321.426	653	318.584	29.988	32.8301	4.767	4.2525	16.236	6.2932	45.452
96	6	15	0	1016	350	565	323.873	565	323.873	26.127	26.1268	4.121	4.5762	15.95	7.0373	52.074
96	7	3	0	1011	363.637	598	327.166	727	320.378	36.471	43.2587	5.064	3.7812	18.758	6.1217	48.618
96	7	4	1	1012	363.093	609	327.582	696	322.031	35.511	41.0621	4.877	5.2516	17.755	6.7749	53.129
96	7	5	1	1019	354.596	618	328.615	700	326.829	25.981	27.7669	4.219	5.3599	17.531	6.6366	46.901
96	7	6	1	1020	355.472	640	332.221	640	332.221	23.251	23.2509	4.877	5.7896	18.642	5.5869	31.767
96	7	9	0	1014	361.495	650	323.204	683	321.64	38.291	39.8554	4.848	5.3967	15.949	6.6005	47.635
96	7	11	1	1011	359.619	602	326.459	602	326.459	33.16	33.1595	5.182	3.0132	17.798	6.057	48.901
96	7	12	0	1015	345.758	536	329.925	454	329.118	15.832	16.6397	4.895	3.7232	13.879	5.8928	36.952
96	7	13	0	1017	358.299	536	333.001	752	328.734	25.298	29.5645	4.629	6.0802	16.24	6.4809	43.14
96	7	16	0	1022	361.413	640	321.589	665	320.657	39.824	40.7558	4.581	4.458	18.538	6.112	44.096
96	7	24	0	1020	359.235	578	325.852	740	320.353	33.383	38.8821	4.572	3.6977	17.851	6.5019	50.971
96	8	17	0	1019	349.331	597	320.92	597	320.92	28.411	28.4105	4.49	1.5579	16.19	6.4588	52.752
96	8	25	0	1018	346.513	646	322.224	661	316.331	24.29	30.1824	4.267	4.1026	12.454	7.1499	52.022
96	8	26	0	1018	349.482	617	321.134	617	321.134	28.348	28.3476	4.197	2.6822	14.376	6.9095	52.982
96	8	27	0	1019	338.827	633	318.993	633	318.993	19.834	19.834	4.566	2.589	12.353	6.1324	41.076
96	8	29	0	1016	351.936	578	322.145	578	322.145	29.791	29.7913	4.616	3.0588	14.031	6.2826	44.79
96	8	30	0	1014	350.916	610	329.324	610	329.324	21.592	21.5919	4.591	4.3555	16.111	6.0532	40.145
96	8	2	0	1017	359.214	614	325.729	614	325.729	33.485	33.4854	4.873	3.4037	17.234	6.3614	50.453
96	8	3	0	1018	356.371	590	326.297	590	326.297	30.074	30.0738	4.6	3.038	15.191	6.3043	46.571
96	8	4	0	1020	362.744	601	324.153	601	324.153	38.591	38.5907	4.598	4.4732	18.965	5.8722	40.828
96	8	8	0	1019	353.357	610	318.671	610	318.671	34.686	34.6858	4.267	2.6136	16.729	6.7164	53.28
96	8	10	0	1016	361.159	514	326.702	743	318.729	34.457	42.43	4.877	4.4521	16.483	6.5698	50.288
96	8	11	1	1017	362.042	559	325.321	559	325.321	36.721	36.7213	4.666	3.5861	17.517	6.644	53.445
96	8	12	0	1017	359.734	550	329.559	770	325.647	30.175	34.0872	4.937	3.7138	17.903	5.8738	42.996
96	8	13	1	1017	371.481	642	324.804	746	320.909	46.676	50.5713	4.531	4.1158	19.675	7.0627	59.567

YR	MO	DY	OCR	MaxPr	MaxThetE	MinPr	MinThetaE	MinPActu	MinTActu	MDPI	DeltaActua	Hm	Qm	Ql	gamma	WI
96	8	14	0	1018	358.475	576	319.983	576	319.983	38.492	38.4923	4.58	1.5737	15.439	6.987	59.682
96	8	15	1	1019	364.471	572	324.352	572	324.352	40.12	40.1196	4.195	4.591	16.912	7.1514	55.027
96	9	2	1	1014	362.696	603	330.381	688	320.783	32.315	41.9129	4.568	4.4808	15.996	6.5674	47.988
96	9	8	0	1014	356.178	563	326.78	563	326.78	29.398	29.3979	4.549	4.8259	15.899	6.5947	47.378
96	9	9	0	1015	348.726	576	331.701	665	330.588	17.025	18.1376	4.373	5.9173	15.033	6.403	39.396
96	9	11	1	1013	366.791	529	329.195	705	322.195	37.596	44.5963	4.485	5.1593	17.972	6.9117	53.394
96	9	16	0	1016	349.785	641	323.18	658	320.584	26.604	29.2005	4.822	2.274	15.312	6.0142	45.183
96	9	17	1	1016	364.991	521	328.501	521	328.501	36.49	36.4901	4.802	6.1974	18.005	6.2472	41.92
96	9	18	1	1015	365.388	555	328.34	555	328.34	37.047	37.0474	5.003	2.9565	18.48	5.9964	48.134
96	9	21	0	1014	353.264	565	321.277	690	315.583	31.988	37.6819	4.286	4.0272	16.096	6.7661	50.523
96	9	22	0	1013	351.084	597	323.38	597	323.38	27.704	27.7044	4.662	4.2083	15.638	6.2206	43.072
96	9	30	0	1020	354.561	649	329.271	700	328.201	25.29	26.3604	4.698	6.1223	16.577	5.9601	34.023
96	9	1	0	1012	354.807	528	324.152	528	324.152	30.655	30.6551	4.78	3.1341	16.413	6.4855	51.514
97	5	19	0	1018	350	604	328.594	604	328.594	21.406	21.406	4.267	5.5419	15.086	6.537	42.251
97	5	20	0	1017	349.787	607	322.405	607	322.405	27.382	27.3818	4.572	2.5553	15.873	6.0095	43.92
97	5	21	0	1016	349.432	575	323.495	657	319.351	25.937	30.0806	4.267	4.5266	15.078	6.6284	46.142
97	5	23	0	1020	342.443	565	320.6	565	320.6	21.842	21.8422	4.615	2.666	14.747	5.4388	32.216
97	5	25	0	1018	341.001	616	317.481	657	315.771	23.52	25.2296	4.612	0.5413	13.117	5.9845	45.364
97	5	26	0	1014	357.243	614	317.224	614	317.224	.40.02	40.0195	4.572	0.4982	16.216	6.8829	61.036
97	5	27	0	1014	350.952	583	320.459	583	320.459	30.493	30.493	4.208	4.7423	15.615	7.3906	56.877
97	5	29	0	1019	339.264	530	323.149	691	321.191	16.116	18.0734	4.185	4.2509	13.386	6.1889	37.144
97	5	30	0	1018	341.354	625	321.203	770	316.18	20.152	25.1748	4.64	1.8073	13.353	6.1423	45.012
97	5	31	1	1014	349.363	596	323.905	596	323.905	25.458	25.4576	4.267	3.9051	14.26	6.4946	44.579
97	6	16	0	1014	340.677	643	319.094	786	314.672	21.583	26.0056	4.898	1.2611	12.565	6.0635	45.369
97	6	17	1	1015	362.638	500	314.68	500	314.68	47.958	47.9576	4.876	3.6598	18.127	6.3502	50.754
97	6	18	0	1019	355.162	632	322.467	632	322.467	32.695	32.6949	4.565	4.0439	15.34	6.5779	48.394
97	6	19	1	1020	351.104	579.8	322.976	579.8	322.976	28.128	28.1281	4.493	2.9401	13.877	6.7216	51.022
97	6	20	0	1019	357.372	555	324.774	555	324.774	32.598	32.5981	4.904	2.2968	15.314	6.4642	52.529
97	6	22	0	1019	349.907	523	322.876	523	322.876	27.032	27.0315	4.546	2.8164	14.039	6.3345	45.893
97	6	23	0	1019	355.007	500	330.071	468	327.72	24.936	27.2876	4.525	5.6946	16.349	6.8286	49.421
97	6	25	0	1020	352.839	638	321.694	638	321.694	31.145	31.1446	4.553	2.1147	14.507	6.3303	48.13
97	6	26	0	1020	355.988	621	323.44	621	323.44	32.548	32.5481	4.57	3.3925	15.464	6.5753	50.036
97	6	27	1	1020	364.368	650	317.641	652.3	317.419	46.727	46.949	4.681	1.1257	18.044	6.4089	56.071

YR	MO	DY	OCR	MaxPr	MaxThetE	MinPr	MinThetaE	MinPActu	MinTActu	MDPI	DeltaActua	Hm	Qm	QI	gamma	WI
97	6	28	0	1018	356.278	647	325.338	714	313.413	30.939	42.8651	4.543	3.9899	15.66	6.4518	46.827
97	6	29	1	1018	350.773	500	313.487	500	313.487	37.286	37.2857	4.442	3.7204	14.901	6.5961	48.256
97	6	4	0	1007	352.403	643	319.711	715	316.165	32.691	36.2374	4.703	1.4529	14.25	5.8898	43.419
97	6	5	0	1007	351.35	643	317.413	785	312.292	33.936	39.0573	4.535	0.5422	13.246	6.0858	46.656
97	6	6	0	1006	352.543	643	316.374	747	314.744	36.17	37.7988	4.427	2.0757	12.924	6.3977	46.697
97	6	1	1	1011	346.611	500	308.892	500	308.892	37.719	37.7194	4.267	4.9961	12.639	6.5651	40.987
97	6	2	1	1009	346.727	593	317.179	593	317.179	29.548	29.5479	4.121	4.5037	13.857	6.5566	42.87
97	6	3	0	1009	332.108	643	315.652	729	309.209	16.456	22.8983	4.423	0.624	8.2637	6.0431	32.104
97	6	10	0	1014	349.349	643	333.309	446	330.928	16.04	18.4207	5.146	5.5773	15.975	5.3931	22.414
97	6	11	0	1015	346.981	581	318.528	581	318.528	28.453	28.4528	4.488	3.84	16.155	5.5483	32.23
97	6	12	1	1012	355.275	622.9	318.605	622.9	318.605	36.67	36.6702	4.655	2.4198	16.33	6.2513	48.927
97	6	13	0	1013	365.234	575	320.012	725	318.967	45.222	46.2672	4.212	3.0365	17.299	7.5735	63.742
97	6	14	1	1015	354.125	629.8	321.35	629.8	321.35	32.775	32.7751	4.267	2.8349	16.297	7.0145	56.411
97	6	15	0	1013	357.947	609	316.672	609	316.672	41.275	41.2751	4.435	0.5156	17.198	6.922	61.472
97	7	1	1	1015	357.228	500	333.3	400	314.295	23.928	42.9333	4.876	5.1503	15.359	6.1517	39.658
97	7	5	1	1016	351.707	614.5	326.503	685	324.015	25.204	27.692	4.717	3.0127	14.264	6.7628	53.171
97	7	6	0	1020	360.49	594	328.779	700	326.889	31.711	33.6015	4.566	4.1298	16.56	6.5704	49.507
97	7	7	0	1022	358.017	643	322.686	828	320.09	35.331	37.9271	4.588	3.1847	14.877	6.7673	52.797
97	7	8	0	1021	356.751	581	322.312	729	320.015	34.439	36.7366	4.592	2.7912	14.905	6.5329	50.258
97	7	10	0	1017	355.159	500	325.835	485	325.539	29.324	29.6205	4.593	4.8259	15.31	6.9671	52.713
97	7	11	0	1019	359.384	540	327.441	540	327.441	31.943	31.9425	4.278	6.2436	14.908	7.2466	51.639
97	7	13	0	1016	353.502	607	321.761	675	315.931	31.741	37.571	4.767	2.446	15.988	6.5029	52.791
97	7	14	0	1017	351.365	643	319.647	746	313.506	31.718	37.8591	4.38	2.3283	16.155	6.3927	49.487
97	7	15	0	1018	357.441	594	321.349	679	318.114	36.092	39.3266	4.396	2.1458	14.913	6.8242	54.666
97	7	17	0	1018	366.612	558	324.687	558	324.687	41.926	41.9255	5.058	1.5309	16.636	5.9314	48.698
97	7	18	0	1009	357.151	578	322.124	654	320.025	35.027	37.1261	4.693	1.3561	16.59	6.1794	50.878
97	7	19	1	1017	355.78	500	313.8	500	313.8	41.98	41.9799	4.364	6.189	14.177	6.9432	46.72
97	7	21	0	1020	350.496	643	335.471	819	332.524	15.026	17.972	4.673	6.0906	14.323	6.206	35.283
97	7	22	0	1019	362.605	650	330.284	650	330.284	32.321	32.3209	5.049	4.7227	17.062	6.1398	43.965
97	7	23	0	1019	378.115	642	334.918	642	334.918	43.198	43.1975	5.507	6.2233	20.699	6.3554	50.663
97	7	26	1	1016	356.334	610	326.004	702	324.708	30.33	31.6261	4.86	2.9225	17.042	6.5638	54.314
97	7	27	1	1016	357.229	500	312.665	500	312.665	44.563	44.5634	4.596	5.5749	16.448	6.9408	51.933
97	7	28	0	1018	351.902	545	325.43	786	324.826	26.471	27.0753	4.839	4.2749	15.396	6.6129	49.893

YR	MO	DY	OCR	MaxPr	MaxThetE	MinPr	MinThetaE	MinPActu	MinTActu	MDPI	DeltaActua	Hm	Qm	Ql	gamma	Wl
97	7	30	0	1019	363.898	542	329.298	689	328.662	34.599	35.2354	4.713	4.8842	16.797	6.5774	48.896
97	7	31	0	1019	356.154	579	325.051	725	323.502	31.104	32.6526	5.231	1.5411	16.678	6.4319	57.138
97	8	16	0	1022	356.967	618	324.611	618	324.611	32.355	32.3553	5.041	2.9512	16.036	6.1495	47.562
97	8	17	0	1022	358.513	580	324.525	488	322.35	33.988	36.1621	4.78	1.8974	17.136	5.8579	45.933
97	8	18	0	1020	356.912	594	328.565	594	328.565	28.347	28.3468	5.23	2.3238	17.371	6.1049	51.129
97	8	20	1	1017	350.536	619.5	324.696	619.5	324.696	25.84	25.84	4.76	4.862	15.531	6.3235	43.353
97	8	21	0	1015	362.585	625	322.681	625	322.681	39.904	39.9044	4.737	3.9164	16.951	6.5444	50.981
97	8	22	0	1013	350.944	531	332.324	451	331.076	18.62	19.8682	4.725	4.5746	14.996	5.9259	35.987
97	8	23	1	1016	346.24	500	315.377	500	315.377	30.864	30.8637	4.876	3.5589	15.268	5.9362	40.398
97	8	24	0	1015	353.7	643	316.402	669	315.763	37.298	37.9366	4.391	1.4187	16.014	6.149	47.998
97	8	25	0	1016	353.901	650	316.724	693	313.487	37.177	40.4143	4.73	2.2425	17	6.3427	51.86
97	8	26	0	1016	349.785	642	318.654	642	318.654	31.131	31.1309	4.514	1.4497	14.433	6.5962	53.162
97	8	1	0	1020	353.31	572	321.951	713	318.311	31.359	34.9985	4.467	3.7785	16.785	5.8203	38.254
97	8	3	1	1020	362.514	500	315.071	500	315.071	47.443	47.4426	4.757	5.2513	16.389	6.5798	47.759
97	8	4	1	1018	361.948	542.7	325.799	400	314.839	36.149	47.1086	4.81	4.4851	15.716	6.4241	46.544
97	8	4	0	1017	360.526	543	326.301	543	326.301	34.226	34.2255	4.803	4.5906	15.373	6.4543	46.296
97	8	5	0	1015	354.467	564	327.673	564	327.673	26.794	26.7939	4.735	3.9232	16.506	5.9133	40.164
97	8	6	1	1016	361.922	587.8	327.476	587.8	327.476	34.446	34.4464	4.876	3.327	15.465	6.0578	43.479
97	8	7	0	1017	357.138	540	323.359	830	323.102	33.779	34.0359	4.74	2.8541	16.915	5.9072	43.682
97	8	8	0	1018	357.129	648	322.053	648	322.053	35.076	35.0757	4.831	5.7848	16.727	6.0028	36.764
97	8	9	0	1018	355.162	515	330.35	465	330.298	24.812	24.8645	5.203	3.2136	15.695	5.98	44.213
97	8	10	1	1019	359.325	522.1	332.827	400	314.243	26.498	45.0815	4.876	5.4197	17.046	6.2334	42.849
97	8	11	0	1020	362.148	611	322.772	671	319.898	39.376	42.2501	4.739	2.6248	14.482	6.1194	44.453
97	8	13	0	1020	360.923	594	323.773	651	323.366	37.15	37.5575	5.163	2.5527	16.011	6.0043	46.783
97	8	15	0	1018	367.193	567	327.053	567	327.053	40.14	40.14	4.943	2.4849	18.78	6.6762	59.222
97	9	3	1	1014	359.71	650	336.376	400	315.801	23.334	43.9083	5.169	5.0338	16.091	6.0747	40.869
97	9	19	0	1017	346.543	643	321.23	705	317.321	25.313	29.2216	5.081	1.415	14.663	6.298	52.256
97	9	26	1	1011	359.88	500	336.449	400	317.761	23.43	42.1182	5.141	5.0721	17.381	5.7187	35.745
97	9	27	0	1011	353.526	565	337.391	565	337.391	16.135	16.1347	5.126	5.1886	16.245	5.0721	14.29
97	9	1	1	1017	348.288	631.9	335.463	631.9	335.463	12.824	12.8243	4.876	5.6553	16.503	5.1745	15.486
98	5	4	1	1013	338.668	550	317.19	785	314.052	21.477	24.616	3.657	3.5681	9.8256	7.2855	43.92
98	5	5	1	1013	340.525	583	311.117	583	311.117	29.408	29.4083	3.509	3.3188	13.214	7.666	55.682
98	5	18	0	1018	337.696	639	318.798	639	318.798	18.898	18.898	4.513	1.3149	10.435	5.8788	34.83

YR	MO	DY	OCR	MaxPr	MaxThetE	MinPr	MinThetaE	MinPActu	MinTActu	MDPI	DeltaActua	Hm	Qm	QI	gamma	WI
98	5	19	0	1017	346.26	643	315.082	865	311.251	31.177	35.0082	5.142	0.3371	14.42	6.1439	52.563
98	5	28	0	1017	358.478	603	335.031	850	324.551	23.447	33.9265	5.152	5.5947	13.948	5.8229	29.299
98	6	18	0	1018	348.704	643	322.921	700	321.317	25.783	27.3869	4.951	1.6463	13.936	6.2615	49.567
98	6	19	0	1017	355.876	572	322.318	572	322.318	33.559	33.5588	4.571	2.3196	13.151	7.4997	63.024
98	6	21	1	1017	357.038	500	310.951	500	310.951	46.087	46.087	4.626	0.5353	15.136	6.3338	52.884
98	6	26	1	1016	357.055	625	315.859	625	315.859	41.196	41.1958	4.595	0.4867	16.689	6.6812	59.05
98	7	5	0	1014	369.171	637	329.081	637	329.081	40.09	40.0896	4.931	4.6723	16.239	6.6923	51.699
98	7	6	1	1015	368.995	521	332.009	483	330.734	36.985	38.2603	4.876	4.7527	17.601	6.893	55.873
98	7	7	1	1016	357.266	641	332.698	400	317.974	24.568	39.2917	4.876	5.151	16.923	6.1383	41.751
98	7	8	0	1018	359.489	643	332.889	700	332.007	26.6	27.4828	4.795	5.3306	16.585	6.2564	42.497
98	7	10	0	1015	355.801	550	331.867	668	330.899	23.934	24.9022	5.162	3.5281	16.705	6.199	48.3
98	7	11	1	1013	366.791	500	316.717	500	316.717	50.074	50.0744	5.299	3.3472	19.875	6.2087	53.652
98	7	12	0	1011	361.79	649	330.613	649	330.613	31.176	31.1764	4.63	4.5116	16.515	6.4796	47.48
98	7	16	0	1018	349.482	594	333.149	716	330.973	16.333	18.5088	5.207	3.5637	14.43	5.7875	37.492
98	7	19	0	1018	356.417	624	328.172	624	328.172	28.245	28.2448	4.884	3.069	14.959	6.3045	47.614
98	7	26	1	1019	362.912	648	321.884	711	319.274	41.028	43.6378	4.876	1.816	16.745	6.5322	56.062
98	7	28	1	1019	358.49	638	322.586	400	316.604	35.903	41.8852	4.572	3.7926	16.854	6.9729	56.462
98	7	29	1	1017	357.948	607	327.747	607	327.747	30.202	30.2016	4.572	5.1758	15.008	6.7567	48.182
98	8	17	1	1020	363.395	621	327.564	621	327.564	35.832	35.8315	4.876	3.4856	17.036	6.3236	49.441
98	8	18	0	1018	353.177	567	328.582	567	328.582	24.595	24.5946	4.56	4.8013	17.143	5.4823	29.427
98	8	19	0	1016	363.775	500	328.513	496	327.712	35.262	36.0624	4.884	4.6309	18.626	6.7281	54.842
98	8	20	0	1017	353.238	650	330.186	650	330.186	23.052	23.0522	4.94	5.4448	16.485	5.6681	30.884
98	8	31	1	1014	355.145	629	328.282	629	328.282	26.864	26.8637	4.863	3.6524	17.028	6.7242	55.062
98	8	1	0	1018	349.365	643	324.34	716	321.242	25.025	28.1228	5.028	5.0861	14.378	6.3644	43.002
98	8	3	0	1016	366.267	554	328.794	554	328.794	37.473	37.4726	4.89	4.6474	18.217	6.7486	54.689
98	8	5	1	1018	364.506	566	324.182	566	324.182	40.324	40.3238	4.468	4.1762	18.824	6.9159	56.224
98	8	6	1	1018	357.596	537	327.465	484	325.328	30.131	32.2684	4.453	5.2716	17.107	6.1532	40.074
98	8	7	0	1018	359.568	643	330.002	656	329.139	29.566	30.4287	4.946	3.7138	17.777	5.8633	42.675
98	8	10	1	1017	371.397	500	312.985	500	312.985	58.412	58.4116	4.876	2.8737	19.676	6.1043	50.825
98	8	12	0	1018	368.468	594	322.208	594	322.208	46.26	46.2595	5.123	0.4748	17.65	6.8318	65.38
98	9	2	0	1011	359.481	642	328.25	642	328.25	31.231	31.231	4.864	3.9927	18.071	5.9622	43.6
98	9	3	1	1008	369.716	500	316.176	500	316.176	53.54	53.5401	4.876	6.419	19.658	6.465	47.637
98	9	4	0	1015	360.332	614	322.031	614	322.031	38.301	38.3011	5.195	0.5611	17.873	5.4564	46.325

YR	MO	DY	OCR	MaxPr	MaxThetE	MinPr	MinThetaE	MinPActu	MinTActu	MDPI	DeltaActua	Hm	Qm	Ql	gamma	Wl
98	9	5	0	1018	358.884	571	329.936	571	329.936	28.949	28.9487	4.897	3.6746	16.813	6.5347	52.093
98	9	6	0	1019	358.146	643	323.403	700	321.806	34.743	36.3401	4.624	4.8424	18.191	6.0552	41.879
98	9	17	0	1014	361.511	603	336.015	654	335.944	25.496	25.5666	4.93	6.3193	18.496	5.4765	26.852
98	9	18	0	1012	360.573	565	337.329	676	336.178	23.244	24.3942	4.84	6.0624	17.316	6.0829	38.408
98	9	19	0	1012	355.956	645	336.055	423	335.867	19.901	20.0883	5.067	5.1415	16.042	5.526	28.24
98	9	21	0	1015	361.912	640	337.672	710	337.462	24.24	24.4497	5.067	5.9525	16.28	5.526	24.942
98	9	22	0	1013	361.789	601	337.741	439	336.938	24.047	24.8502	5.191	5.389	17.859	5.6337	33.831
98	9	26	0	1017	371.922	645	333.474	645	333.474	38.448	38.4479	4.709	6.1223	20.89	6.1586	44.171
98	9	1	0	1012	368.246	591	326.679	591	326.679	41.566	41.5662	4.498	4.7932	15.234	7.1144	54.343

Appendix F: Pearson Correlation Coefficient (*r*) Table

STUDENT EDITION OF STATISTIX 12/21/99, 2:04:22 PM

CORRELATIONS (PEARSON)

	OCCUR	HM	MDPI	DELTAACTU	GAMMA	MINPACTUA	MINPRES
HM	-0.0583						
MDPI	0.2385	0.0415					
DELTAACTU	0.2636	0.1336	0.8505				
GAMMA	0.2010	-0.5052	0.3540	0.3001			
MINPACTUA	-0.3196	-0.0833	-0.0701	-0.0996	0.0824		
MINPRES	-0.3418	-0.0942	-0.2237	-0.2134	-0.0234	0.6399	
QL	0.0548	0.4661	0.4072	0.3803	-0.2189	-0.1603	-0.2120
QM	0.1321	-0.0511	-0.2159	-0.1572	-0.0662	-0.3535	-0.3106
WI	0.0899	-0.0698	0.5863	0.5264	0.7753	0.2067	0.0418
MAXTHETAE	0.1846	0.5080	0.6224	0.6272	0.0075	-0.1971	-0.2233
MINTHACTU	-0.1263	0.3781	-0.3786	-0.5568	-0.3598	-0.0882	0.0234
MINTHETAE	-0.0944	0.4888	-0.5563	-0.3693	-0.4229	-0.1239	0.0352

	QL	QM	WI	MAXTHETAE	MINTHACTU
QM	0.2745				
WI	0.0330	-0.5209			
MAXTHETAE	0.8017	0.2058	0.2488		
MINTHACTU	0.3889	0.4122	-0.3799	0.2977	
MINTHETAE	0.3555	0.4813	-0.4495	0.3041	0.7770

CASES INCLUDED 100 MISSING CASES 0

Appendix G: Discriminant Analysis Input Table for Training Data

Number	Occur	DeltaActua	MinPActua	Gamma
1	1	30.5078	535	6.13497
2	1	30.6852	614	6.79737
4	1	35.6141	627	6.74633
6	1	25.5138	477	5.44959
8	1	24.4132	545	5.58444
10	1	34.9978	628	6.84346
11	1	42.0995	561	6.54879
12	1	28.8326	463	5.95483
13	1	32.9438	705	6.56406
14	1	27.5195	603	5.78737
15	1	34.4821	700	6.26058
18	1	27.2448	703	5.67293
19	1	37.194	678	6.27436
20	1	31.7443	541	6.61184
22	1	29.1636	666	5.99342
25	1	27.7669	700	6.63658
27	1	33.1595	602	6.05701
31	1	41.9129	688	6.56737
32	1	44.5963	705	6.91173
33	1	36.4901	521	6.24724
34	1	37.0474	555	5.99642
35	1	29.5479	593	6.55659
36	1	42.9333	400	6.15171
37	1	37.7194	500	6.56514
38	1	12.8243	631.9	5.17449
39	1	45.0815	400	6.23343
40	1	36.6702	622.9	6.25134
41	1	32.7751	629.8	7.01451
42	1	47.9576	500	6.35015
43	1	41.9799	500	6.94317
44	1	28.1281	579.8	6.72157
48	1	42.1182	400	5.71873
49	1	44.5634	500	6.94082
50	1	46.949	652.3	6.40889
51	1	37.2857	500	6.59613
52	1	47.4426	500	6.57978
53	1	43.9083	400	6.07468
54	1	25.4576	596	6.49458
56	1	27.692	685	6.76277
57	1	34.4464	587.8	6.05782
58	1	58.4116	500	6.10432
59	1	50.0744	500	6.20872
60	1	35.8315	621	6.32357

Number	Occur	DeltaActua	MinPActua	Gamma
61	1	46.087	500	6.33377
62	1	43.6378	711	6.53218
63	1	41.1958	625	6.68118
69	1	40.3238	566	6.91585
70	1	29.4083	583	7.666
71	1	32.2684	484	6.15315
72	1	38.2603	483	6.89302
1	0	39.1073	739	6.09223
9	0	27.9205	574	6.55219
11	0	36.8882	500	6.30631
15	0	32.5415	615	5.98687
19	0	26.2678	545	6.1672
23	0	43.6061	500	6.43821
24	0	31.4046	804	5.66572
25	0	33.76	537	5.93245
27	0	39.4521	500	5.68543
28	0	38.441	741	6.85841
29	0	35.7476	690	6.3762
32	0	23.5493	601	6.21611
43	0	16.6397	454	5.89278
47	0	26.1268	565	7.0373
50	0	29.2005	658	6.01418
58	0	38.8821	740	6.50185
62	0	28.3476	617	6.90954
70	0	26.3604	700	5.96013
72	0	43.2587	727	6.12171
75	0	39.8554	683	6.60046
76	0	18.1376	665	6.40298
77	0	38.5907	601	5.87224
80	0	27.3818	607	6.0095
82	0	28.4528	581	5.54828
85	0	26.0056	786	6.06353
87	0	32.5981	555	6.46421
88	0	30.0806	657	6.62836
90	0	27.2876	468	6.82864
95	0	40.0195	614	6.88285
97	0	42.8651	714	6.45184
98	0	25.1748	770	6.14228
100	0	36.2374	715	5.88978
101	0	39.0573	785	6.08584
107	0	26.7939	564	5.91333
113	0	37.8591	746	6.39273
115	0	39.3266	679	6.82418
116	0	32.3553	618	6.14947
118	0	41.9255	558	5.93137
121	0	29.2216	705	6.29795

Number	Occur	DeltaActua	MinPActua	Gamma
124	0	19.8682	451	5.92591
125	0	32.3209	650	6.13981
131	0	32.6526	725	6.43193
138	0	37.9366	669	6.14901
142	0	31.1764	649	6.4796
144	0	25.5666	654	5.47652
145	0	24.5946	567	5.48232
152	0	20.0883	423	5.52596
159	0	31.231	642	5.96217
161	0	40.0896	637	6.69228
163	0	36.3401	700	6.0552

Appendix H: Discriminant Analysis Input Table for Verification

Number	Occur	DeltaActu	MinPActu	Gamma
3	1	36.8599	723	6.33855
5	1	34.2638	571	6.38257
7	1	29.8398	697	7.10294
9	1	31.9383	700	6.57558
16	1	40.1619	615	6.67788
17	1	40.3701	585	6.20586
21	1	24.6991	519	7.13066
23	1	34.9947	621	7.02293
24	1	41.0621	696	6.77486
26	1	23.2509	640	5.58692
28	1	36.7213	559	6.64398
29	1	50.5713	746	7.06269
30	1	40.1196	572	7.15143
45	1	25.84	619.5	6.32353
46	1	30.8637	500	5.93617
47	1	31.6261	702	6.56379
55	1	47.1086	400	6.42412
64	1	41.8852	400	6.97294
65	1	30.2016	607	6.75672
66	1	53.5401	500	6.46495
67	1	26.8637	629	6.72424
68	1	24.616	785	7.28548
73	1	39.2917	400	6.13829
26	0	48.1011	630	5.91607
34	0	41.2154	693	5.90926
39	0	29.3167	491	5.81623
44	0	32.8301	653	6.29317
46	0	38.4923	576	6.98701
49	0	25.2333	509	6.05282
53	0	28.3034	560	6.71272
54	0	37.6819	690	6.76606
55	0	33.1985	649	6.26208
57	0	38.1181	598	6.08861
69	0	30.7538	582	6.68811
71	0	30.0738	590	6.30429
74	0	38.8438	733	7.0528
78	0	42.43	743	6.56977
79	0	18.0734	691	6.18891
86	0	32.6949	632	6.57792
102	0	37.7988	747	6.39768
106	0	34.0359	830	5.90724
112	0	37.571	675	6.50294
117	0	36.1621	488	5.8579

Number	Occur	DeltaActu	MinPActu	Gamma
119	0	28.3468	594	6.10491
122	0	39.9044	625	6.54437
126	0	43.1975	642	6.3554
127	0	31.1309	642	6.59615
128	0	16.1347	565	5.07206
130	0	35.2354	689	6.57738
136	0	36.7366	729	6.53293
137	0	24.8645	465	5.97998
139	0	37.4726	554	6.7486
140	0	24.9022	668	6.19904
141	0	46.2595	594	6.83183
143	0	18.5088	716	5.78753
146	0	18.898	639	5.87884
154	0	41.5662	591	7.11438
160	0	38.3011	614	5.4564
162	0	28.9487	571	6.53472
164	0	30.4287	656	5.86334
165	0	27.4828	700	6.25637
166	0	24.8502	439	5.63372

Appendix I: Discriminant Analysis Mathcad Template

ORIGIN ≡ 1

This is a template that uses output from S-Plus 2000 to determine the cut-off between microburst occurrence and non-microburst occurrence.

$$xbar_1 := \begin{bmatrix} 36.29817 \\ 571.37 \\ 6.380975 \end{bmatrix} \quad xbar_2 := \begin{bmatrix} 32.17186 \\ 632.90 \\ 6.2083707 \end{bmatrix}$$ These are the group means.

$$S_{pooled} := \begin{bmatrix} 58.16686 & -11.764 & .847691 \\ -11.764 & 8488.621 & 6.187427 \\ .847691 & 6.187427 & .180611 \end{bmatrix}$$ Pooled Sample Variance Covariance Matrix

$b_{hat} := S_{pooled}^{-1} \cdot (xbar_1 - xbar_2)$ This computes the discriminant vector (weights).

$$b_{hat} = \begin{bmatrix} 0.055 \\ -7.876 \cdot 10^{-3} \\ 0.966 \end{bmatrix}$$ s the discriminant vector (sample approximations of discriminant weights)

$Cutoff := b_{hat}^{T} \cdot \frac{(xbar_1 + xbar_2)}{2}$ This computes the cuttoff

Cutoff = (3.231)

x :=

A:\verify62.txt

DeltaActual := $x^{\langle 9 \rangle}$ MinPActual := $x^{\langle 6 \rangle}$ Γ := $x^{\langle 13 \rangle}$

$Y := b_{hat_1} \cdot DeltaActual + b_{hat_2} \cdot MinPActual + b_{hat_3} \cdot \Gamma$ This is the discriminant function

Y =

	1
1	2.466
2	3.563
3	3.022
4	2.604
5	3.827
6	3.619
7	4.166
8	3.828
9	3.333
10	1.642
11	4.045
12	3.743
13	4.621
14	2.658
15	3.503
16	2.56

Cutoff = (3.231)

The first 23 are microburst days the second 39 are non-microburst days

References

Atkins, N. T., and R. M. Wakimoto, 1991: Wet-microburst activity over the southeastern United States: Implications for forecasting, *Weather and Forecasting*, **6**, 470-482.

Brown, J. M., K. R. Knupp, and F. Caracena, 1982: Destructive winds from shallow, high-based cumulonimbi. Preprints, *12th Conference on Severe Local Storms*, San Antonio, American Meteorological Society, 272-275.

Byers, H. R., and R. R. Braham, 1949: The Thunderstorm. Washington: U.S. Department of Commerce, Weather Bureau.

Caracena, F., J. R. McCarthy, and J. Flueck, 1983: Forecasting the likelihood of microbursts along the front range of Colorado. Preprints, *13th Conference on Severe Local Storms*, Tulsa, American Meteorological Society, 261-264.

-----, F., and M. Maier, 1987: Analysis of a microburst in the FACE meteorological Mesonetwork in southern Florida. *Monthly Weather Review*, **115**, 969-985.

-----, R. L. Holle, and C. A. Doswell III., 1990: Microbursts a Handbook for Visual Identification (Second Edition). Washington: U.S. Government Printing Office.

Dillon, W.R., and M. Goldstein, 1984: Multivariate Analysis Methods and Applications. New York: John Wiley and Sons

Doswell, C. A. III, 1994: Extreme convective windstorms: Current understanding and research. *Report of the Proceedings of the U.S.-Spain Workshop on Natural Hazards*, Barcelona, Spain, University of Iowa, 44-55.

Devore, J.L., 1995: Probability and Statistics for Engineering and the Sciences (Fourth Edition). Cincinnati: Duxbury Press

Duffield G.F., and G.D. Nastrom, 1983: Equations and Algorithms for Meteorological Applications in Air Weather Service. AWS/TR-83/001, Scott AFB, IL: Air Weather Service

Ellrod, G.E., and J.P. Nelson III, 1998: Experimental Microburst Image Products Derived from GOES Sounder Data. unpublished article, http://orbit35i.nesdis.noaa.gov/arad/fpdt/fpdt_pubs/wf98mb.html

Fujita, T.T., and F. Caracena, 1977: An analysis of three weather-related aircraft accidents. *Bulletin of the American Meteorological Society*, **58**, 1164-1181.

-----, 1985: The downburst microburst and macroburst. SMRP Res. Pap., No. 210, University of Chicago, [NTIS PB-14880]

Kachigan, S.K, 1986: Statistical Analysis: An Interdisciplinary Introduction to Univariate and Multivariate Methods. New York: Radius Press

Kachigan, S.K., 1991: Mulitivariate Statistical Analysis: A Conceptual Introduction (Second Edition). New York: Radius Press

Ladd, J. W., 1989: An introductory look at the south Texas downburst. NOAA Tech. Memo., NWS SR-123, Scientific Services Division, NWS Southern Region, Fort Worth, TX, 19 pp.

McCann, D. W., 1994: WINDEX - a new index for forecasting microburst potential. *Weather and Forecasting*, **9**, 532-541.

-----, Experimental Forecast Facility, National Severe Storms Forecast Center, Kansas City, MO. Personal Correspondences, December 1999

Murdoch, G., 1997: Forecasting Dry Microburst Potential Using the WINDEX unpublished article. http://www.srh.noaa.gov/ftproot/topics/attach/html/ssd97-6.htm

Raytheon, 1996: Eastern Range Instrumentation Handbook. Computer Sciences Raytheon Range Technical Services Contract Number F08650-94-C-0001

Roeder, W. P., Chief Staff Meteorologist, 45th Weather Squadron, Patrick AFB FL. Personal Correspondences. February - December 1999.

Rogers, R.R., and M.K. Yau, 1996: A Short Course in Cloud Physics (Third Edition).Woburn, MA: Butterworth-Heinemann

Sanger, N.S., 1999: A Four-Year Summertime Microburst Climatology and Relationship Between Microbursts and Cloud-to-Ground Lightning Flash Rate for the NASA Kennedy Space Center, Florida: 1995-1998. MS thesis, Texas A&M University

Sohl, C. J., 1987: West Texas dry microburst of 21 May 1986. NOAA Tech. Memo., NWS SR-121, Scientific Services Division, NWS Southern Region, Fort Worth, TX, 1-9.

Stewart, S. R., 1991: The prediction of pulse-type thunderstorm gusts using vertical integrated liquid water content (VIL) and the cloud top penetrative downdraft mechanism. NOAA Tech. Memo. SR-136, Scientific Services Division, NWS Southern Region, Fort Worth, TX, 20pp.

Wakimoto, R. M., 1985: Forecasting dry microburst activity over the High Plains. *Monthly Weather Review*, **113**, 1131-1143.

-----, and V. N. Bringi, 1988: Dual-polarization observations of microbursts associated with intense convection: The 20 July storm during the MIST project. *Monthly Weather Review*, **116**, 1521-1539.

Wallace, J.M., and P.V. Hobbs, 1977: Atmospheric Science: An Introductory Survey. New York: Academic Press

Wheeler, M.M., and W. P. Roeder, 1996: Forecasting wet-microbursts on the Central Florida Atlantic Coast in support of the United States Space Program. Preprints, *18th Conference on Severe Local Storms*, San Francisco, American Meteorological Society, 654-658.

Wilks, D.S., 1995: Statistical Methods in the Atmospheric Sciences. New York: Academic Press

Wolfson, M. M., 1990: Understanding and predicting microbursts. *Proceeds of the 16th Conference on Severe Local Storms*, Kananaskis Park, AB, Canada, American Meteorological Society, 340-351

Vita

Captain Steven N. Dickerson was born in Pt. Pleasant, New Jersey on 11 August 1971. He graduated from Brick Township High School in 1989 and enrolled at Rutgers University in New Brunswick, New Jersey. He graduated with a Bachelor of Science degree in Meteorology in May 1993, receiving a commission through the Air Force Reserve Officers Training Corps (ROTC).

In September 1993, Captain Dickerson was assigned to the 12th Air Support Operations Squadron, Fort Bliss, Texas where he served as the Regimental Staff Weather Officer to the 3rd Armored Cavalry Regiment. In November 1994, he was assigned to the 18th Weather Squadron, Fort Bragg, North Carolina where he served as the Special Operations Forces Weather Flight Commander providing weather support to the U.S. Army's 3rd and 7th Special Forces Groups (Airborne). Captain Dickerson was later assigned to Detachment 5, 10th Combat Weather Squadron also on Fort Bragg. He entered the School of Engineering and Management, Air Force Institute of Technology in August 1998. His follow-on assignment is to the United States Air Forces Europe (USAFE) Operational Weather Squadron, Sembach, Germany.

Captain Dickerson is married to the former Diane Guedes of Manahawkin, New Jersey. They have two children, Kevin and Amanda.

REPORT DOCUMENTATION PAGE	Form Approved OMB No. 0704-0188

1. AGENCY USE ONLY *(Leave blank)*	2. REPORT DATE	3. REPORT TYPE AND DATES COVERED
	March 2000	Master's Thesis

4. TITLE AND SUBTITLE
An Evaluation of Microburst Prediction Indices for the Kennedy Space Center and Cape Canaveral Air Station (KSC/CCAS)

5. FUNDING NUMBERS

6. AUTHOR(S)
Steven N. Dickerson, Captain, USAF

7. PERFORMING ORGANIZATION NAME(S) AND ADDRESS(ES)
Air Force Institute of Technology
Graduate School of Engineering and Management (AFIT/EN)
2950 P Street, Building 640
WPAFB OH 45433-7765

8. PERFORMING ORGANIZATION REPORT NUMBER
AFIT/GM/ENP/00M-06

9. SPONSORING/MONITORING AGENCY NAME(S) AND ADDRESS(ES)
45th Weather Squadron
Attn: Mr. William P. Roeder
1201 Edward H. White II St., MS 7302
Patrick AFB, FL 32925-3238 DSN 467-8410

10. SPONSORING/MONITORING AGENCY REPORT NUMBER

11. SUPPLEMENTARY NOTES
Advisor: Lt Col Cecilia A. Miner, ENP, DSN: 785-3636, ext. 4645

12a. DISTRIBUTION AVAILABILITY STATEMENT
APPROVED FOR PUBLIC RELEASE; DISTRIBUTION UNLIMITED.

12b. DISTRIBUTION CODE

13. ABSTRACT *(Maximum 200 words)*

A microburst event on 16 August 1994 at the Kennedy Space Center's (KSC) Shuttle Landing Facility alerted forecasters from the 45th Weather Squadron (45WS), the provider of weather support to the KSC and Cape Canaveral Air Station (CCAS), to the challenges of microburst prediction. Although there was no operational impact, this event caused the 45WS to revise their thunderstorm forecasting procedures to specifically address microbursts, resulting in the locally developed Microburst-Day Potential Index (MDPI). MDPI provides a several-hour outlook of microburst potential based on the results of the Microburst and Severe Thunderstorm (MIST) project. The 45WS also conducted a preliminary evaluation of the Wind INDEX (WINDEX) for the KSC/CCAS microburst forecast problem. WINDEX estimates the maximum observed gust speed that can be expected should a microburst occur.

This thesis presents an evaluation of MDPI and WINDEX. A new microburst potential index is also introduced, incorporating both the MDPI and WINDEX parameters. Overall neither the MDPI nor the WINDEX performed particularly well. MDPI showed very little improvement over random guessing, and WINDEX showed very little correlation to observed microburst gust speeds. The new microburst potential index generally outperformed MDPI. Further refinement of the new index is needed to make it more useful operationally.

14. SUBJECT TERMS	15. NUMBER OF PAGES
Microbursts, Wet-Microbursts, Downbursts, Downdrafts, Fujita, Discriminant Analysis, WINDEX	98
	16. PRICE CODE

17. SECURITY CLASSIFICATION OF REPORT	18. SECURITY CLASSIFICATION OF THIS PAGE	19. SECURITY CLASSIFICATION OF ABSTRACT	20. LIMITATION OF ABSTRACT
UNCLASSIFIED	UNCLASSIFIED	UNCLASSIFIED	UL